Can kinematic (or “ordinary” dynamics) be responsible for exotica ?

Role of kinematic reflections

Adam Szczepaniak (Indiana U.)

Characteristics of peripheral production

Have we seen a exotic meson yet

5q sightings

Kinematic reflections
Ghosts

The goal of amplitude analysis is to identify dynamical effects (bound states, resonances, channel couplings). These appear as singularities of scattering amplitude.

There is no unique "formula" for the scattering amplitude (not even for pi-pi elastic scattering ! Do scalar resonances bootstrap to the cross channel?)

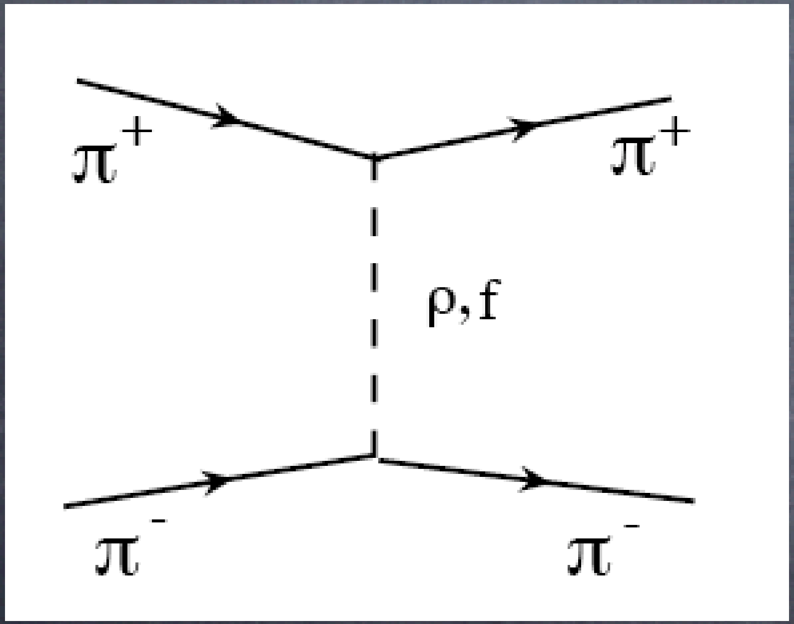

rho and f's have to add coherently and suppress u-channel reggions at all s and t (FESR)

There are only (often incompatible) constraints (or "truths") : analyticity, crossing relations, unitarity.

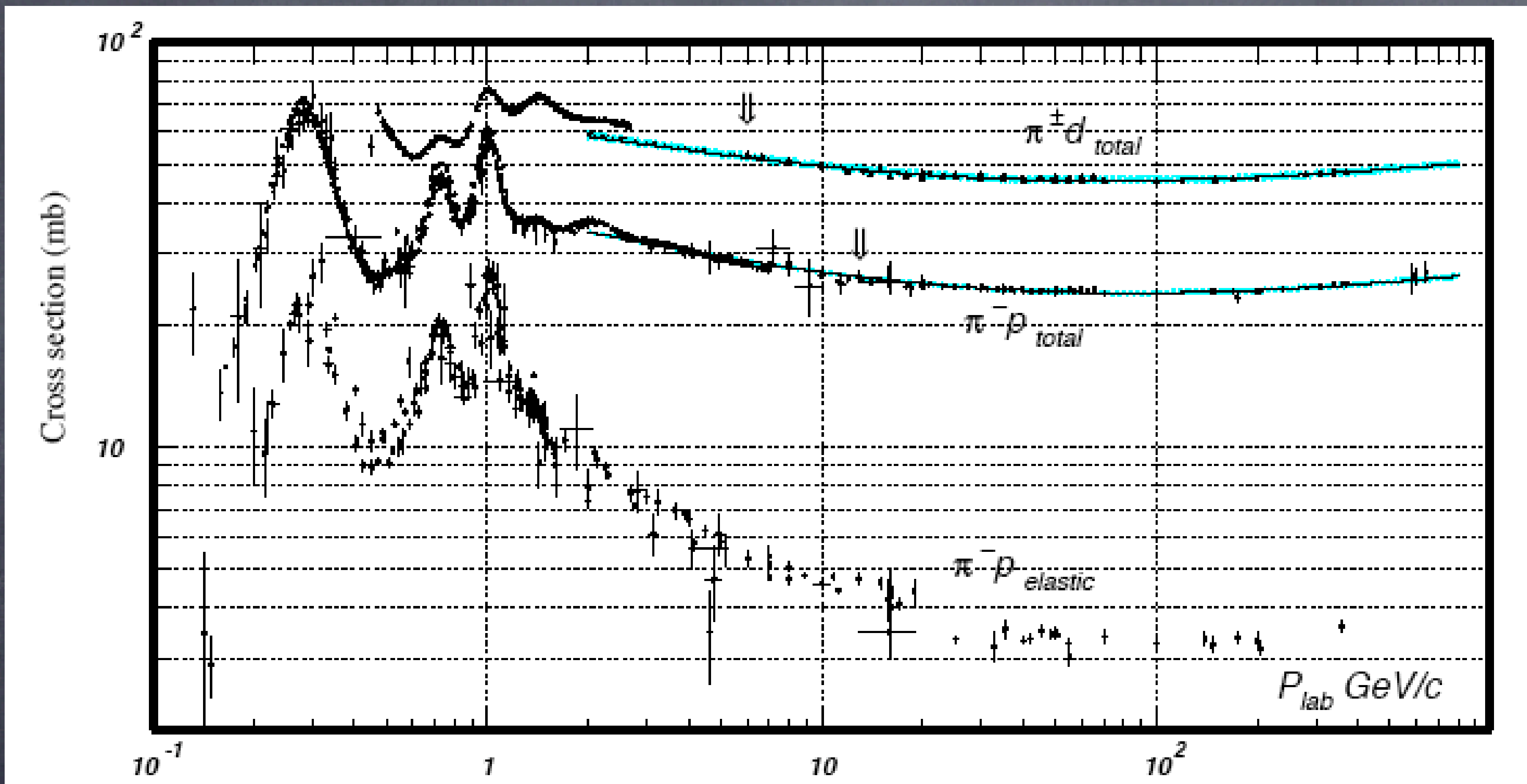

Cross section (mb)
10^2
10
10^-1
1
10
10^2
π^± d total
π^- p total
π^- p elastic
P lab GeV/c

Analyticity : $A(s,t,\cdots) \underset{s>>t}{\longrightarrow} f(t)s^{\alpha(t)}$

unitarity limit: $\alpha(t \le 0) \le 1$

s-t crossing: $\alpha(t) \leftrightarrow J_t$

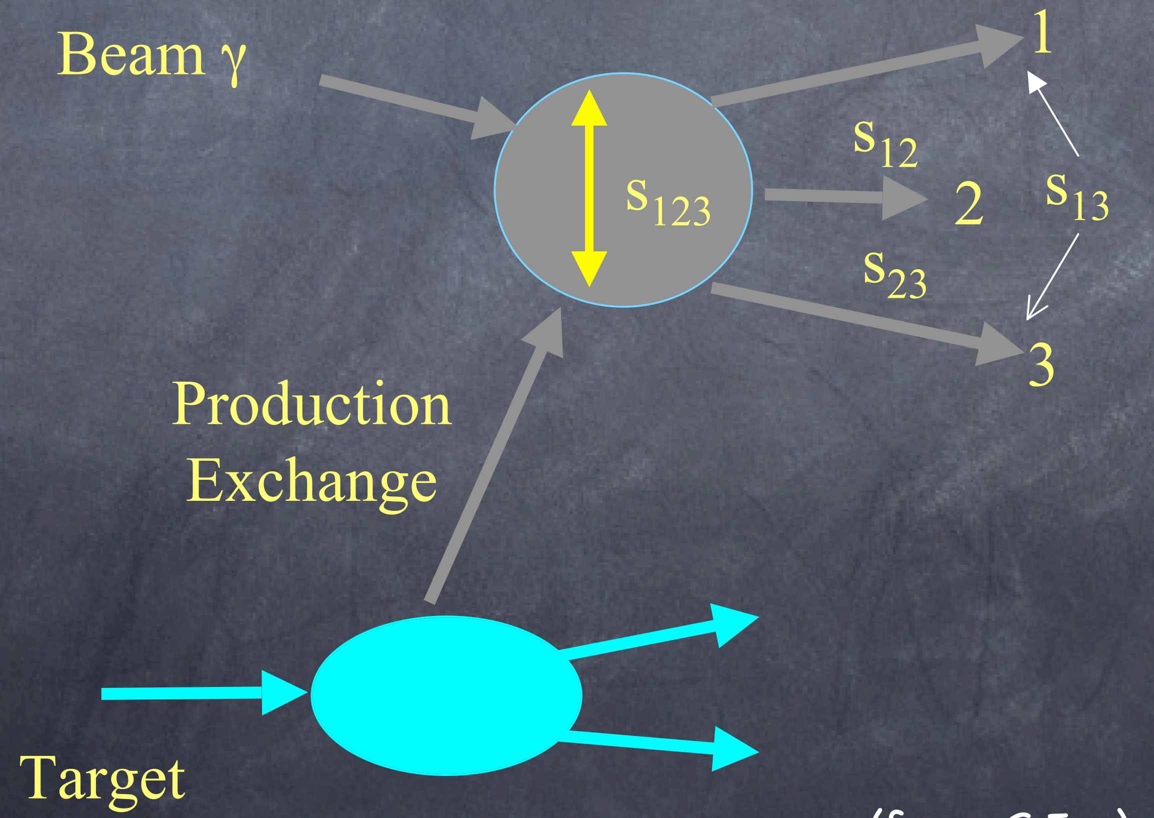

(from G.Fox)

$\pi^- p \to \pi^0(\eta) n$ (dashed)

$\pi^- p \to \pi^0(\eta) X$ (solid)

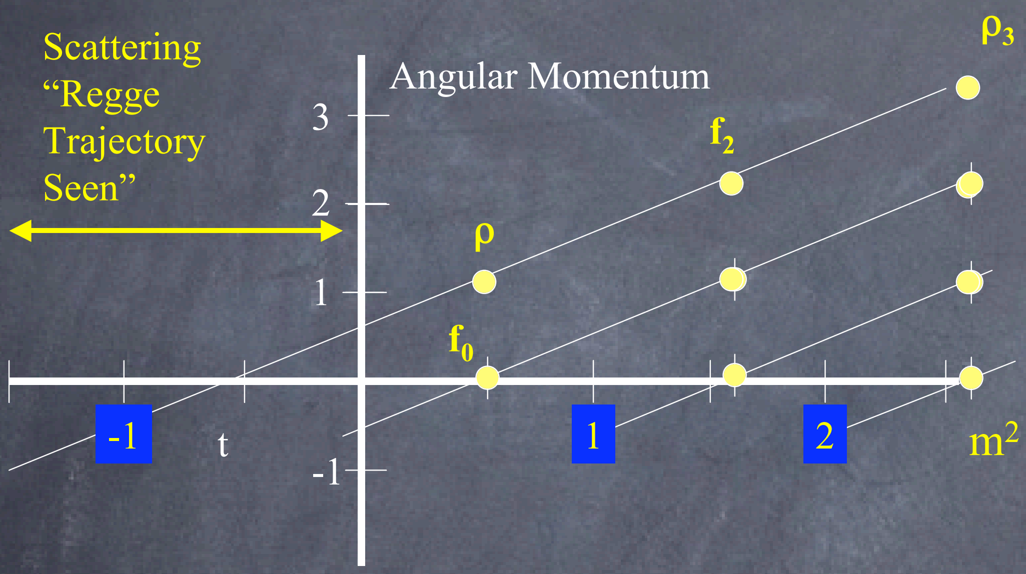

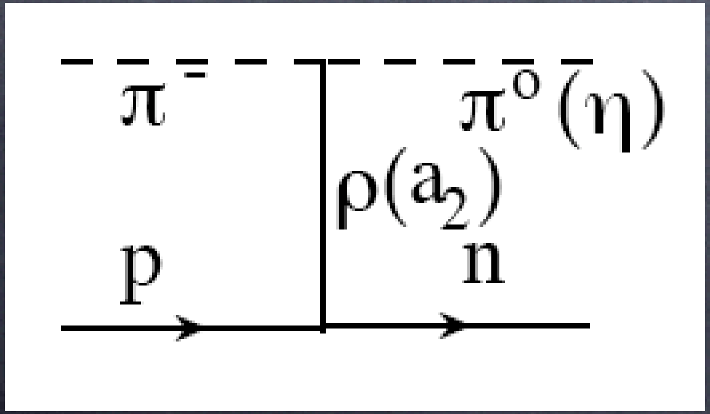

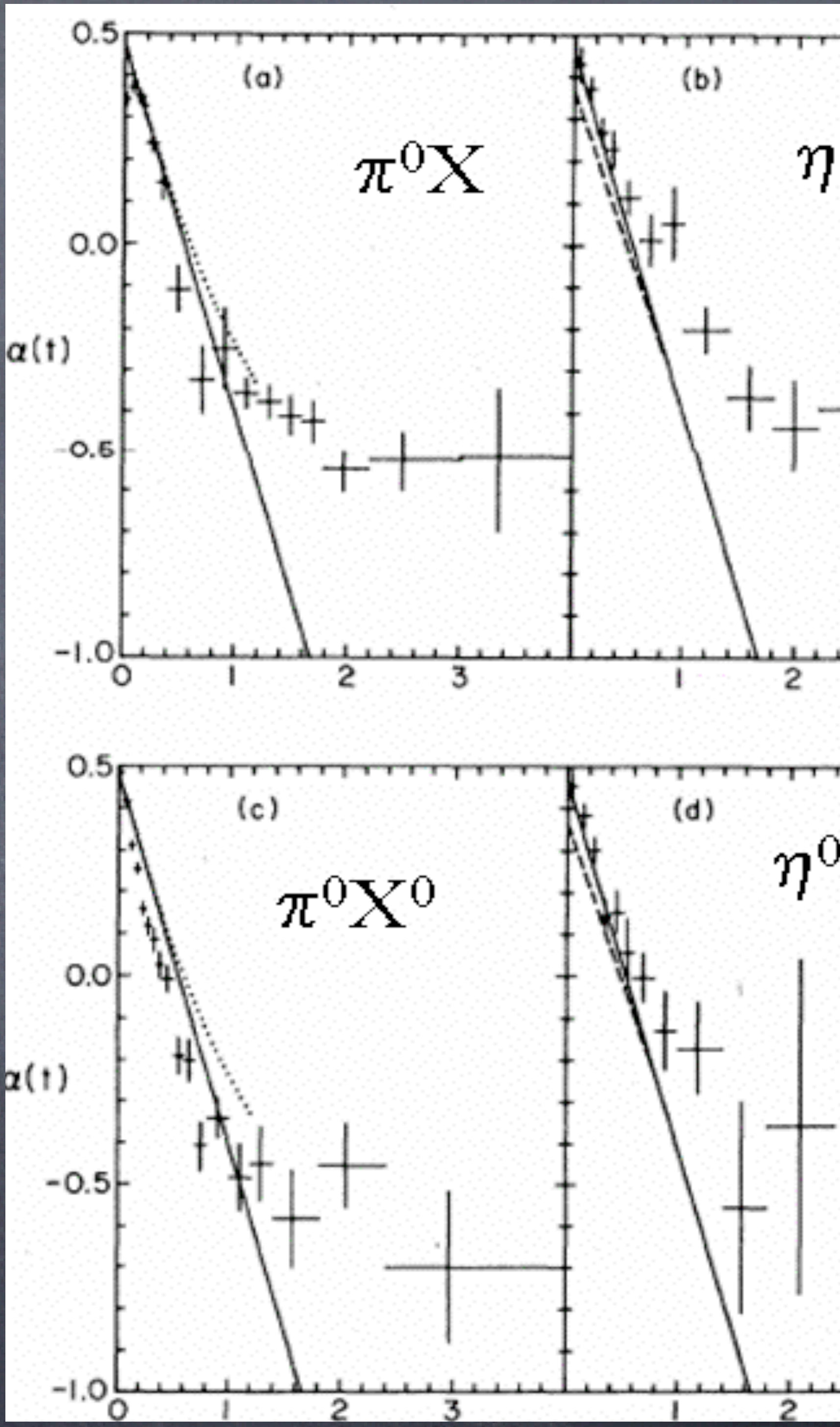

Classic EXD argument is based on absence of 5q (<Im A> over low s = Im A at high s)

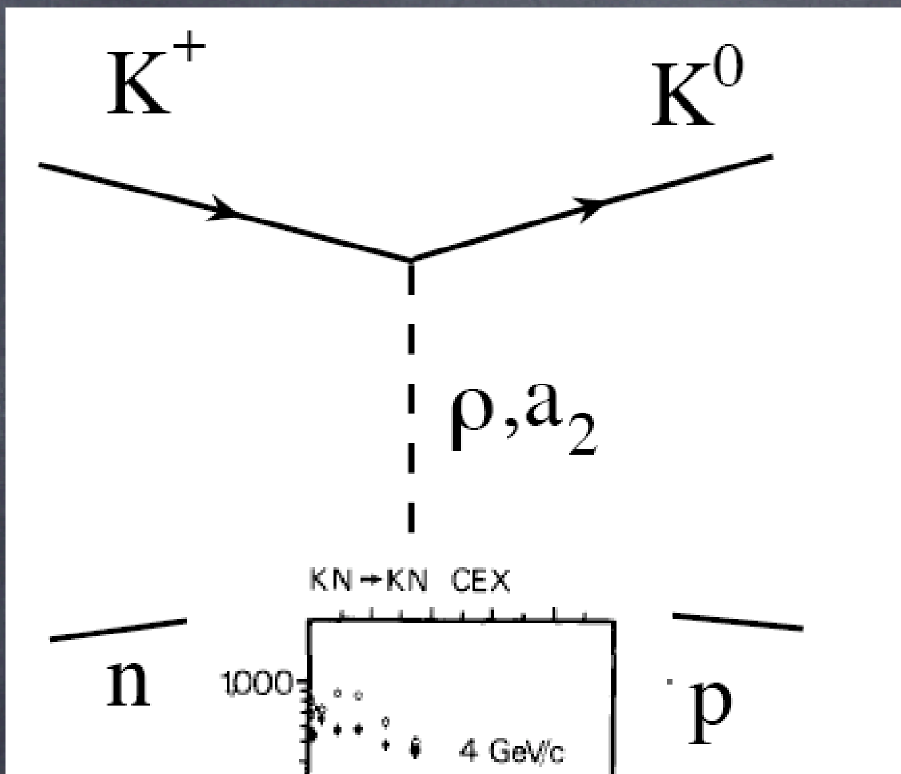

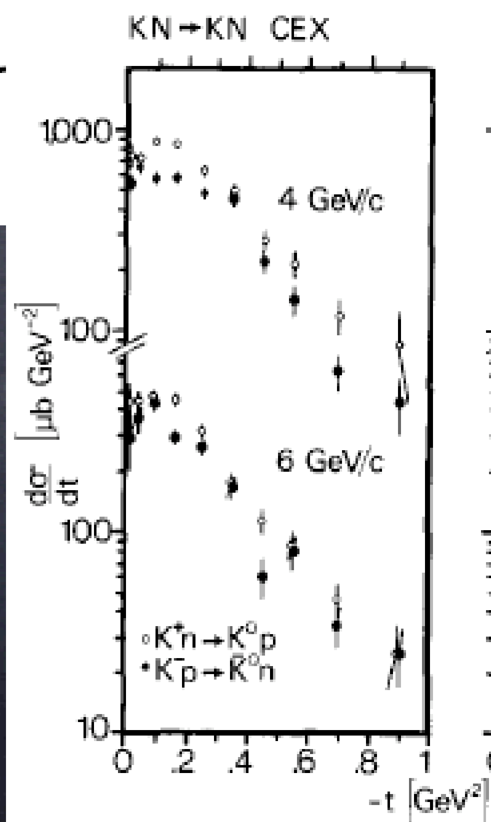

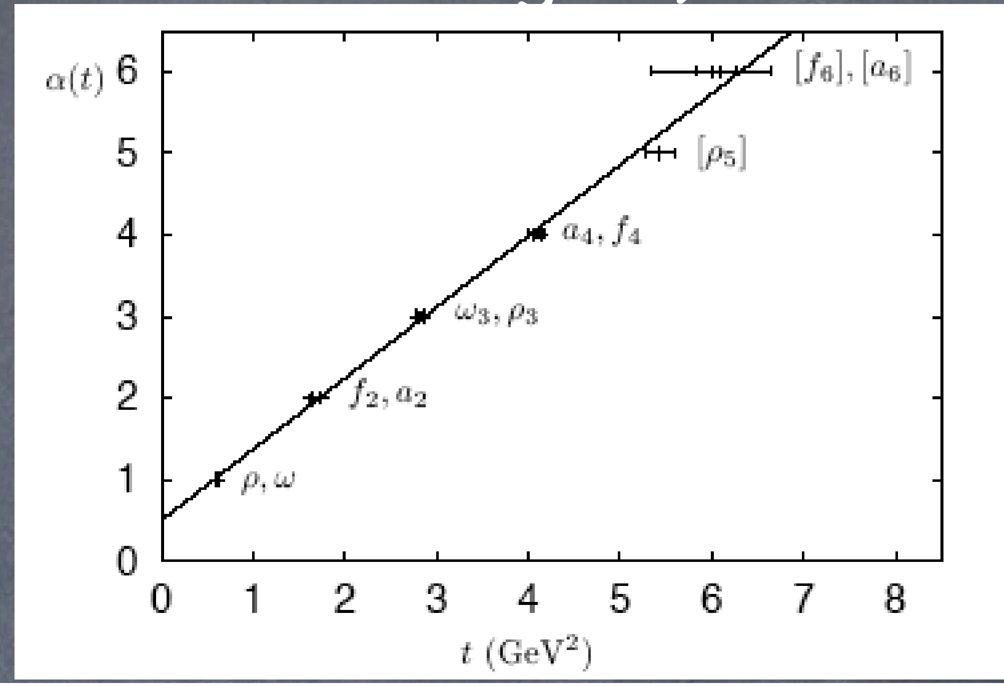

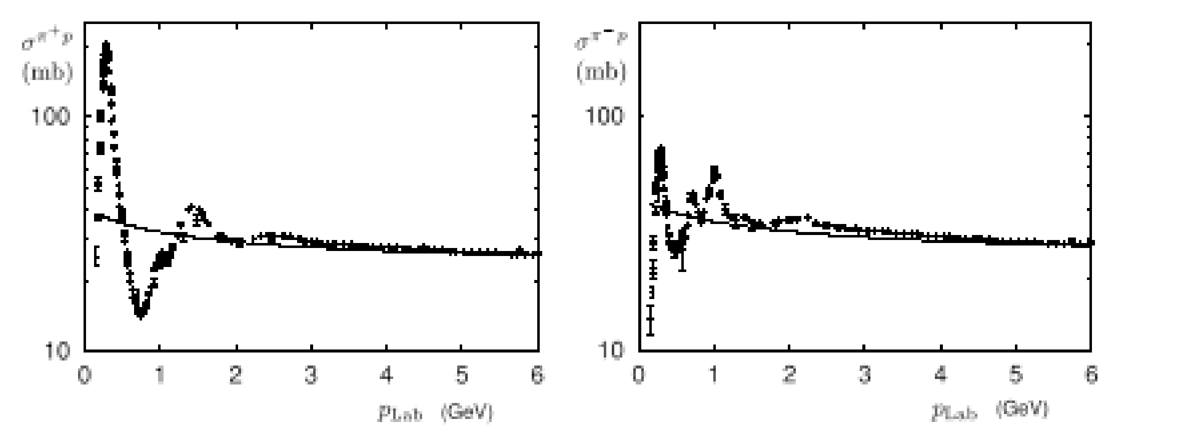

FIG. 6. Total π^+p (left plot) and π^-p (right plot) cross sections as a function of laboratory momentum, $p_{\rm Lab}$, compared with Regge fits to high energy data. (Adapted from Ref. [18].)

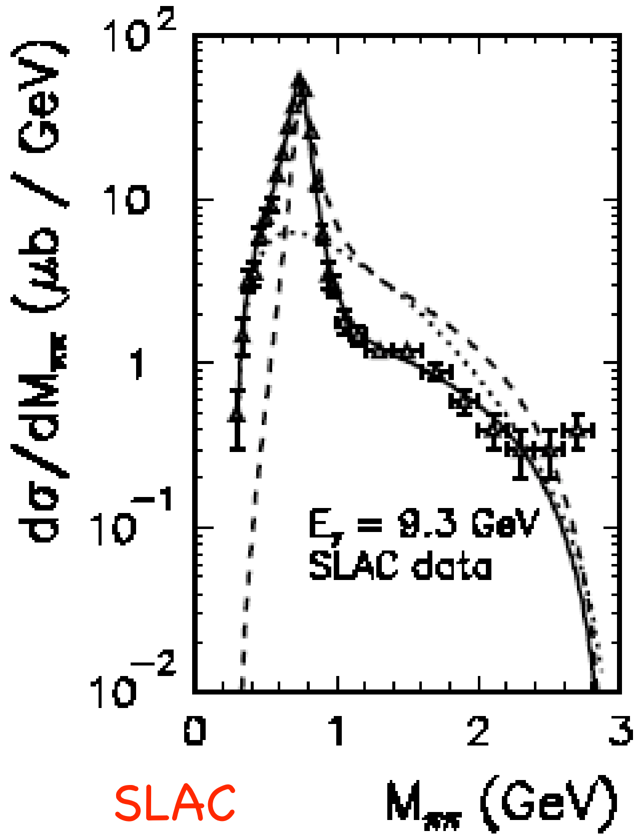

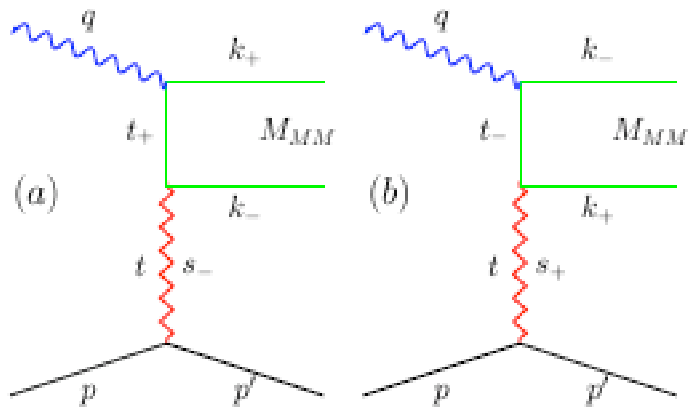

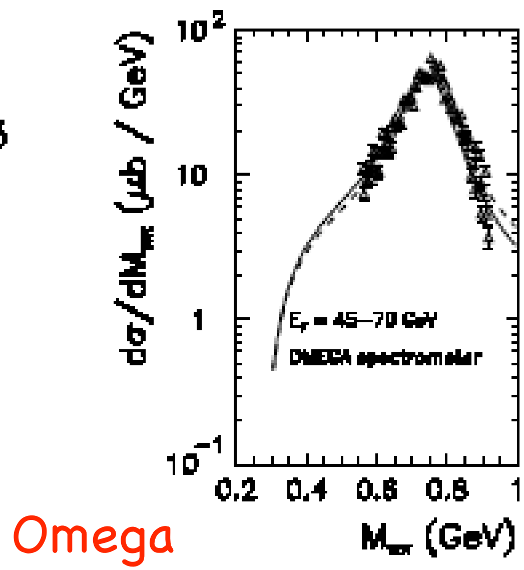

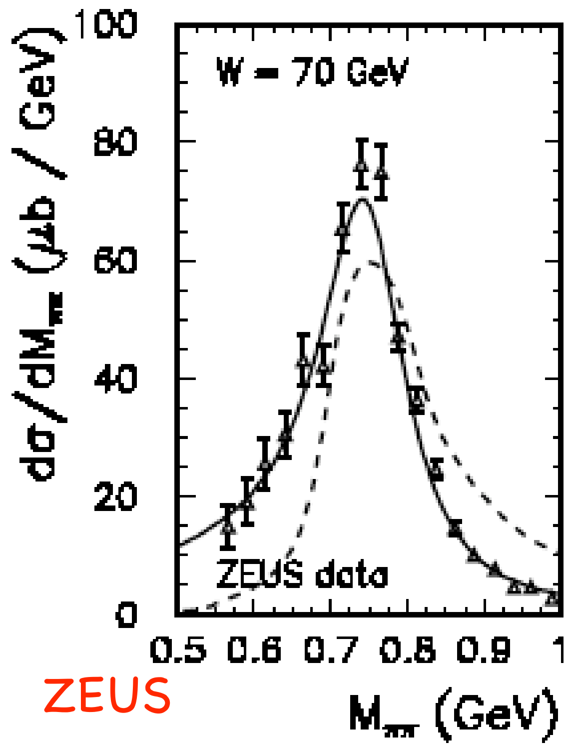

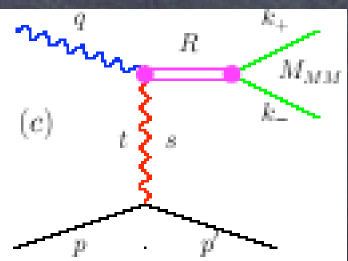

$$\gamma p \to \pi^+ \pi^- p$$

$\gamma(3-8\ \text{GeV})p \to K\bar{K}p$

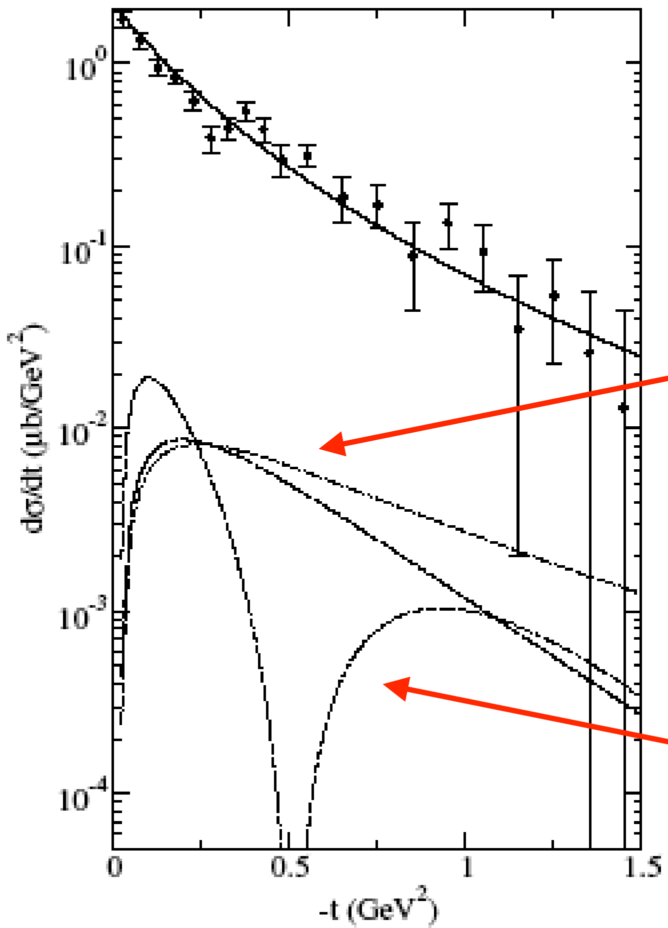

Fig. 2. Differential cross section at $E_\gamma = 4$ GeV. The solid line shows the model t-distribution for the ϕ photoproduction, the dotted line is the P-wave contribution with $M = 0$ multiplied by the branching ratio of the ϕ decay into the K^+K^- pair. The dashed line is the S-wave part of the K^+K^- cross section calculated for normal ρ, ω propagators, while the double dotted-dashed line corresponds to the Regge propagators. Model parameters are given in Table 1. The data are from Fig. 6b of [18]

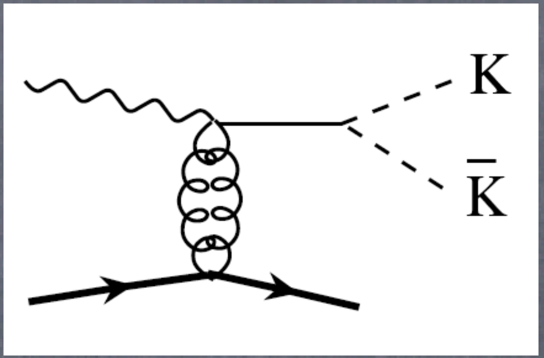

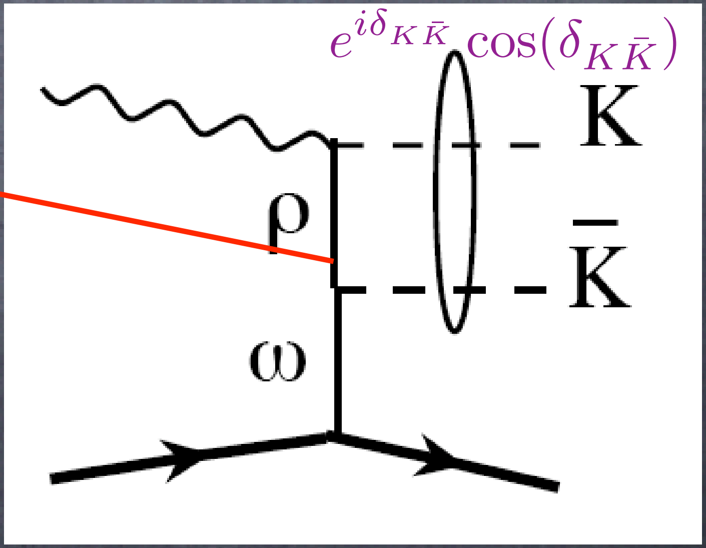

data: Daresbury & DESY

Regge vs elementary particle exchange
(pion exchange)

PHYSICAL REVIEW D VOLUME 48, NUMBER 7 1 OCTOBER 1993

Further results from charge-exchange photoproduction

G. T. Condo, T. Handler, W. M. Bugg, G. R. Blackett, M. Pisharody, and K. A. Danyo
Department of Physics, University of Tennessee, Knoxville, Tennessee 37996-1200
(Received 3 August 1992; revised manuscript received 1 March 1993)

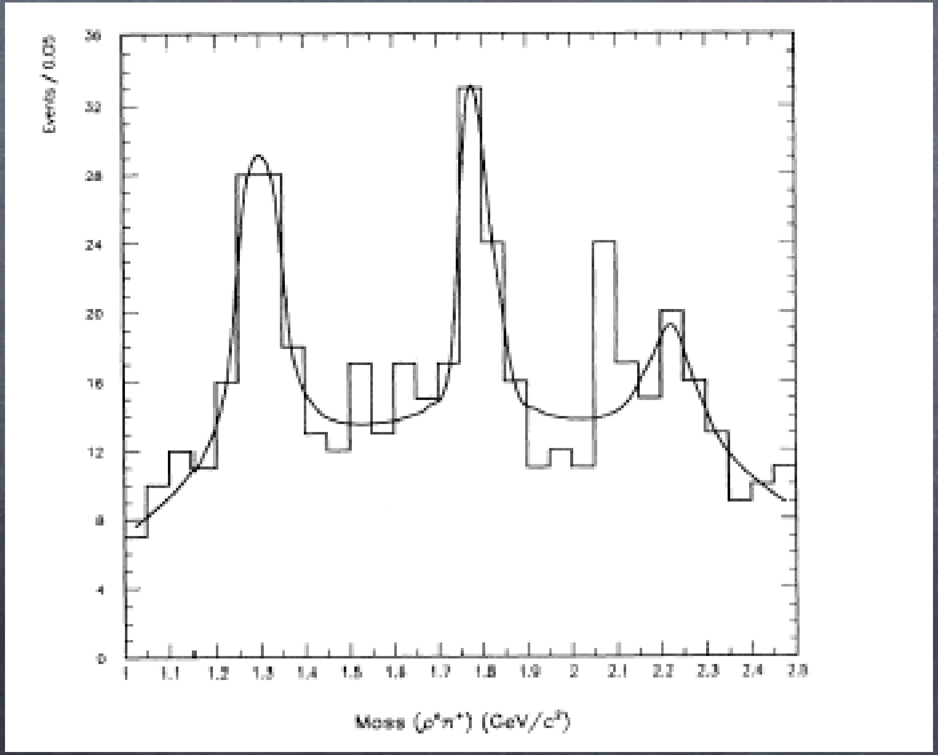

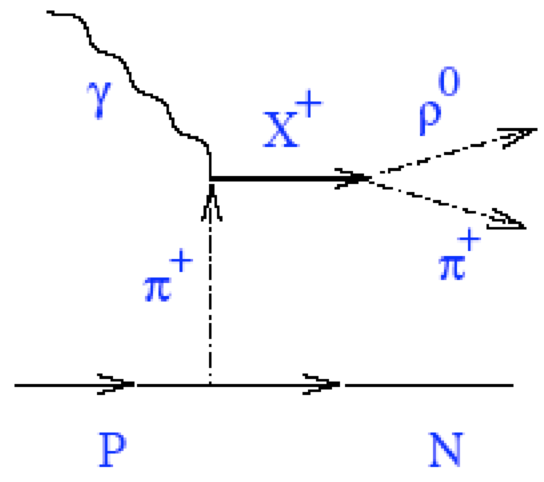

Fig. 1. $\rho^0\pi^+$ photoproduction via one-pion-exchange.

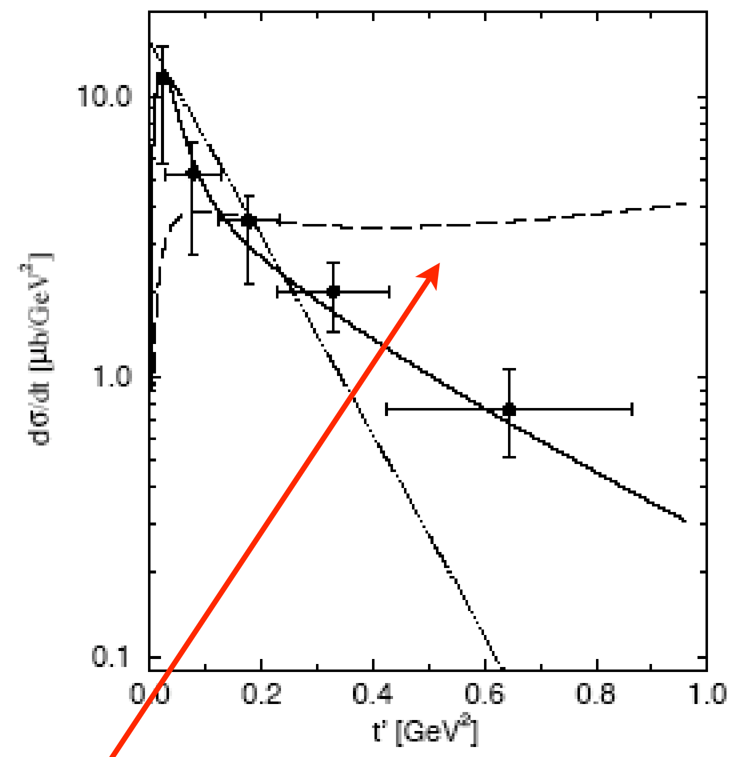

$$\frac{d\sigma}{dt}(\gamma p \rightarrow A_2{}^+ n) = \frac{\pi}{64}\,\frac{g_{\pi NN}{}^2}{4\pi}\,\frac{g_{A\pi\gamma}{}^2}{4\pi} \times \frac{1}{m_A{}^6 k^2 s}\,\frac{|t|(t-m_A{}^2)^4}{(t-\mu^2)^2},$$

Three is no known method
for "fine tuning"
Regge theory

Fig. 3. Momentum transfer dependence of a_2^+ photoproduction cross section. Data is from Ref. [15]. Solid line is the OPE prediction corrected to account for absorption. Dashed line is the pure OPE prediction and the dotted line is the $A\exp(-bt)$ parameterization.

Exotic mesons: 1^{-+}

Exciting (exotic) meson resonances

E852: $E_\pi = 18\text{GeV}$

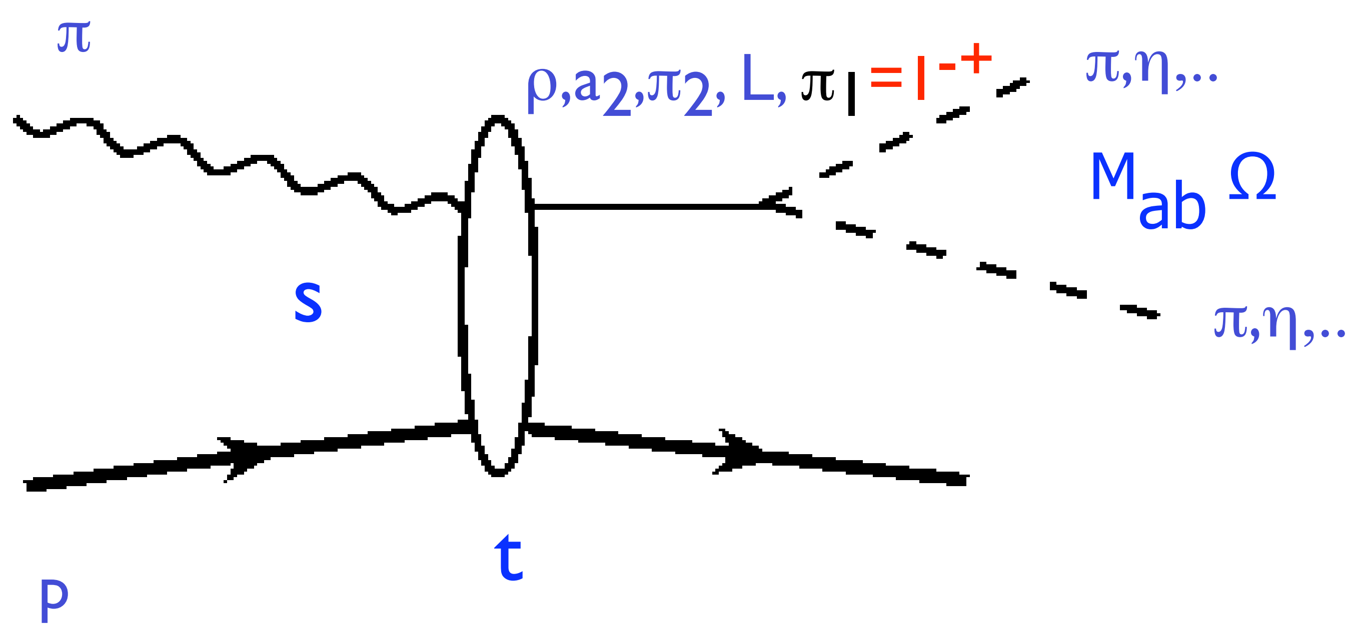

Peripheral production on the "meson cloud"

It is important to determine dependence on all kinematical variables, $s,t,M_{ab}\ \Omega$

Exotic story

$\pi^- p \to \eta \pi^0 N$
$\to \eta \pi^- p$

$(\eta\pi^0)$ in P-wave has $J^{PC}=1^{-+}$!

$$\pi^- p \to \eta \pi^- p$$

$M = 1370 \pm 16^{+50}_{-30}$ MeV / c^2

$\Gamma = 385 \pm 40^{+65}_{-105}$ MeV / c^2

BNL (E852)
Confirmed by
Crystal Barrel similar mass, width

$$\pi^- p \to \eta \pi^0 n$$

Mass dependent P-wave present in $\eta\pi^0$ (E852)

New results: No consistent resonance interpretation for the P-wave

$$\pi^- p \to \eta' \pi^- p$$

$M = 1597 \pm 10^{+45}_{-10}$ MeV / c^2

$\Gamma = 340 \pm 40^{+50}_{-50}$ MeV / c^2

(E852)

P-wave strong and unambiguous: need to focus on interpretation

$$\pi^- p \to \rho^0 \pi^- p$$

$M = 1593 \pm 8^{+29}_{-47}$ MeV / c^2

$\Gamma = 168 \pm 20^{+150}_{-12}$ MeV / c^2

(E852) Confirmed by VES

Disappears in the full data sample !

$M = 1709 \pm 24 \pm 41$ MeVc^2

$\pi^-\pi^-\pi^+\eta = f_1\pi^-$ $\quad \Gamma = 403 \pm 80 \pm 115$ MeVc^2

$\pi^+\pi^-\pi^-\pi^0\pi^0 = b_1\pi^-$ $\quad \Gamma = 185 \pm 25 \pm 28$ MeVc^2

More from (E852)

Have we seen exotic mesons
The $\pi_1(1400)$ story

$$I(\Omega) = |SY_{00}(\Omega) + \sum_m P_m Y_{1m}(\Omega) + \cdots|^2$$

$$I(\Omega) \to I_{exp.}(\Omega) = I(\Omega)\ \text{acceptance}\ (\Omega)$$

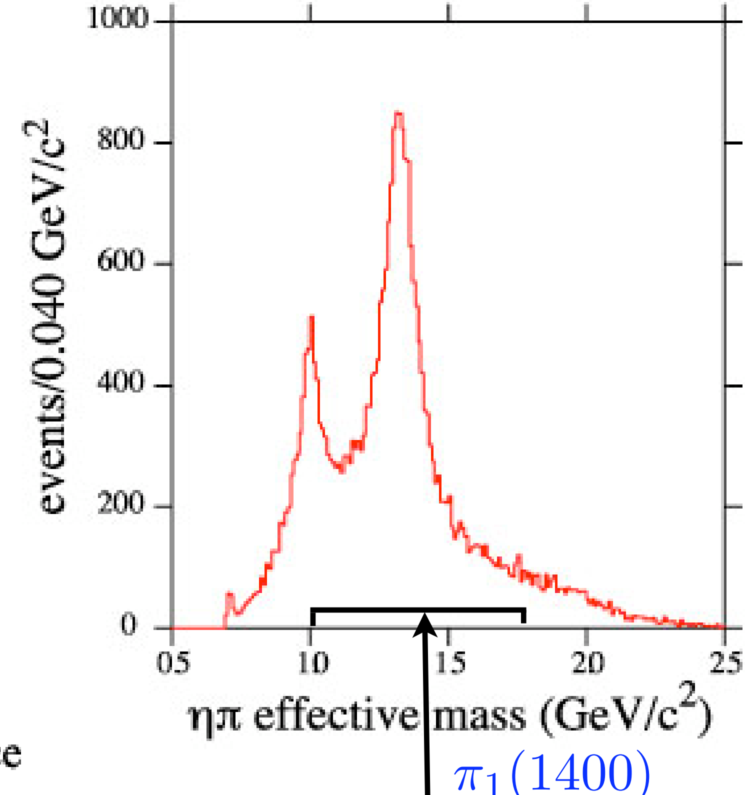

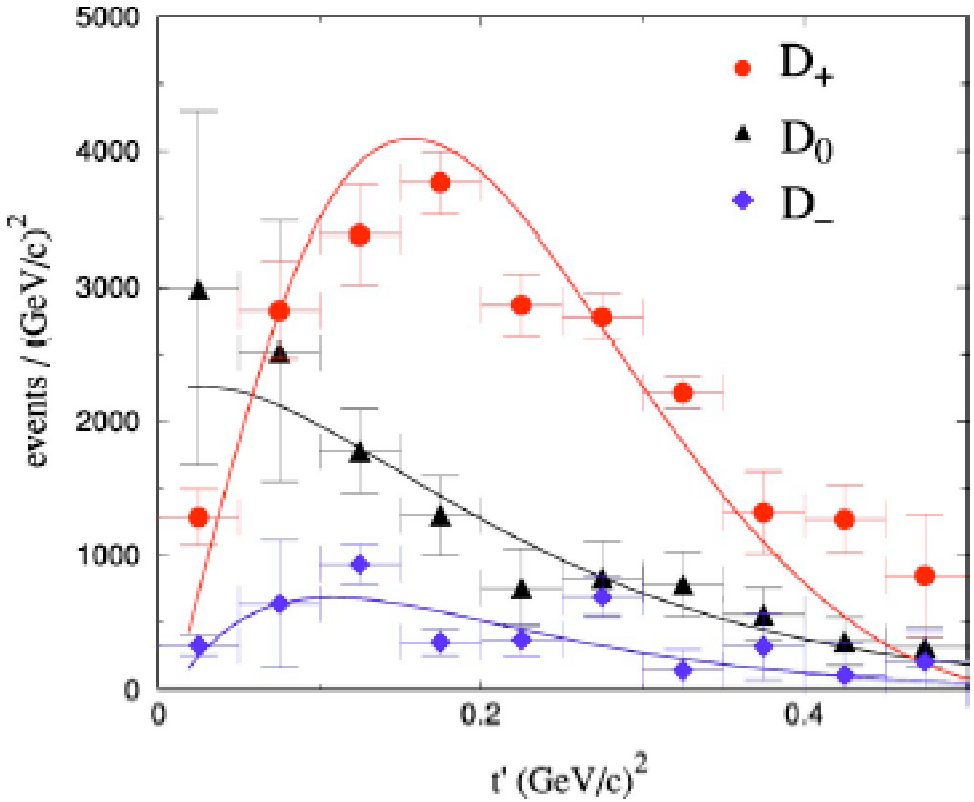

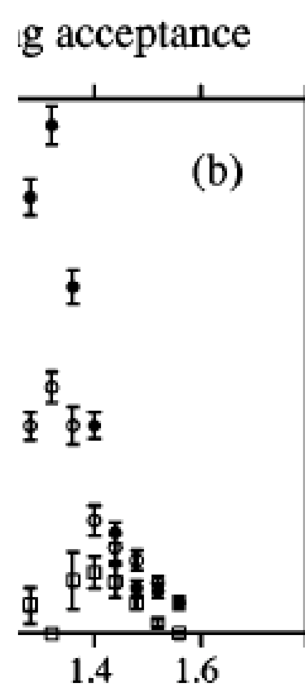

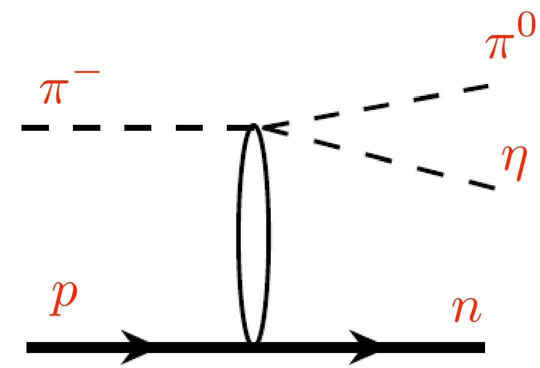

$H_{10} \sim Re[P_+ D_+^*]$

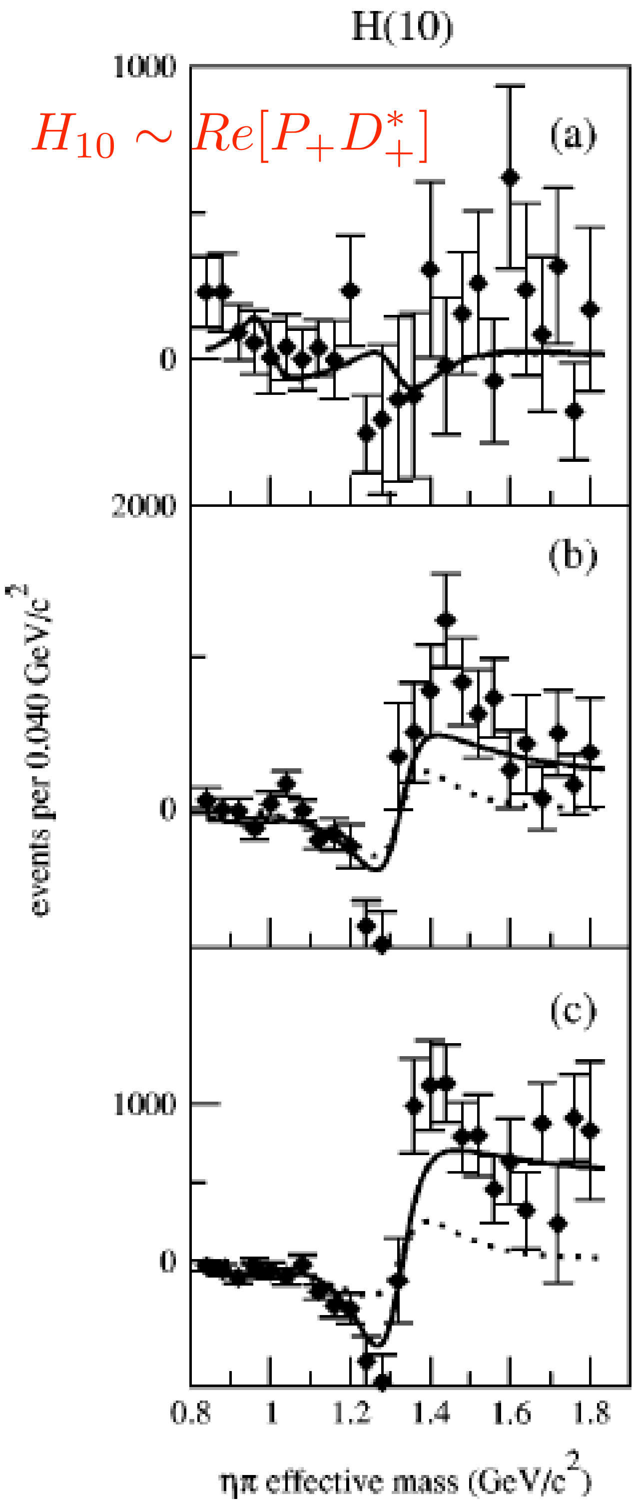

$P_m = P_+, P_-, P_0$

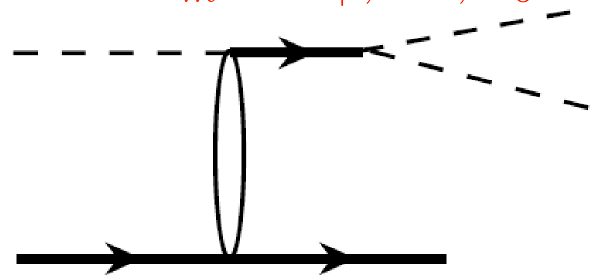

$H_{11} \sim Re[S_0 P_0^*], Re[P_0 D_-^*]$
$Re[P_- D_0^*]$

Assume BW resonance
in all, m=+1,0,-1 P-waves

$\pi_1(1400) \to \pi_1(900 - 5000)!$

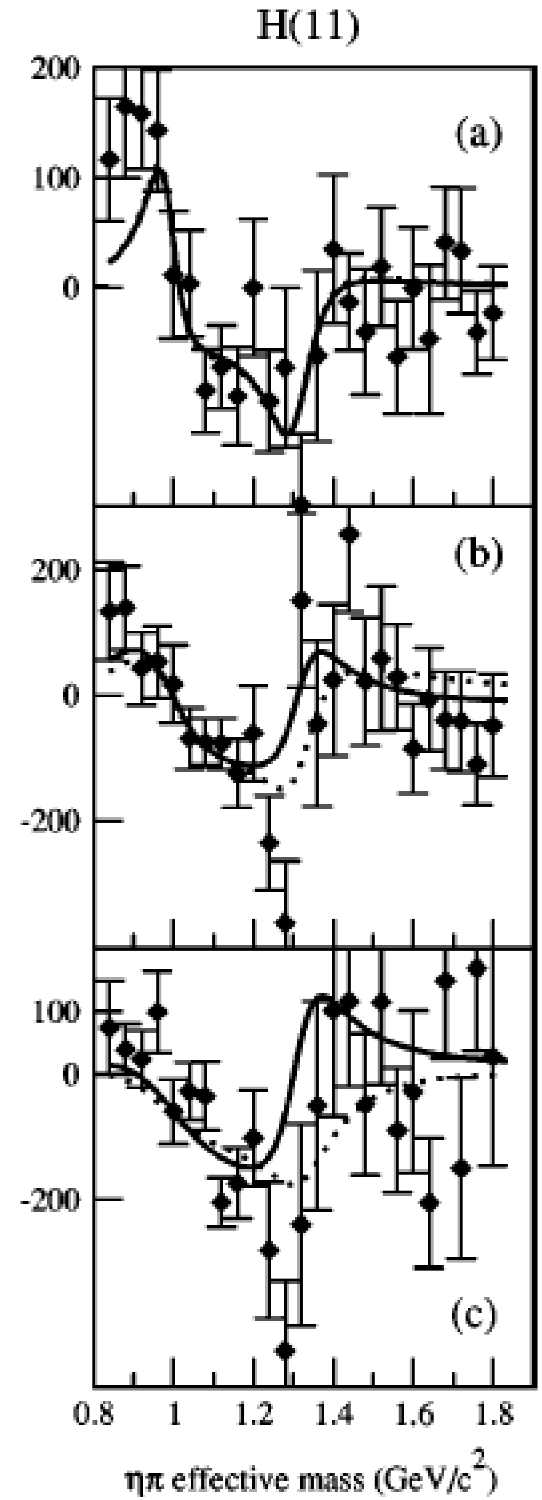

Clear P-wave in $\eta'\pi$

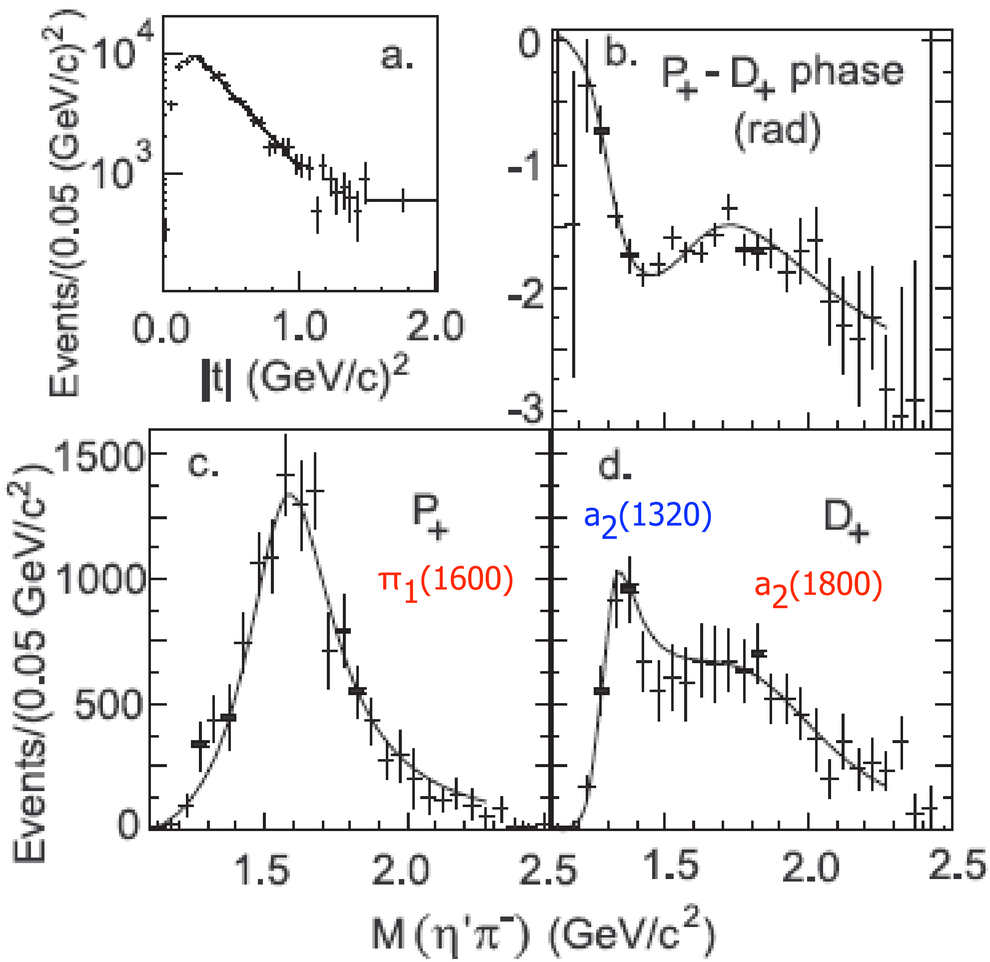

$\pi^- p \to \pi^-\pi^+\pi^- p$

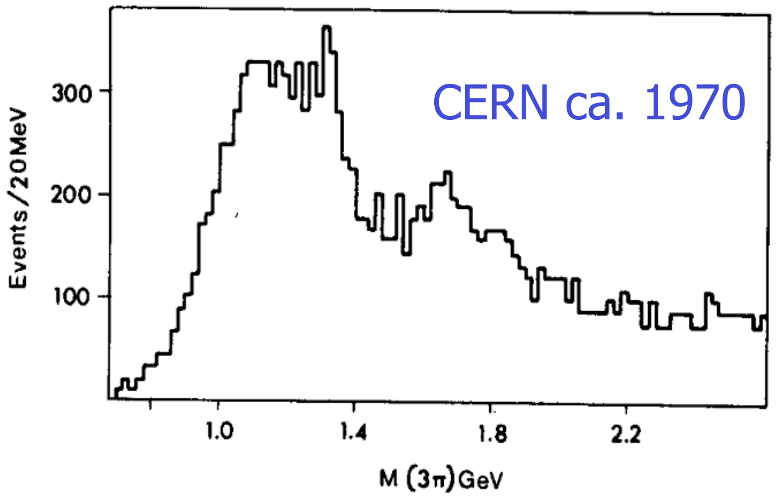

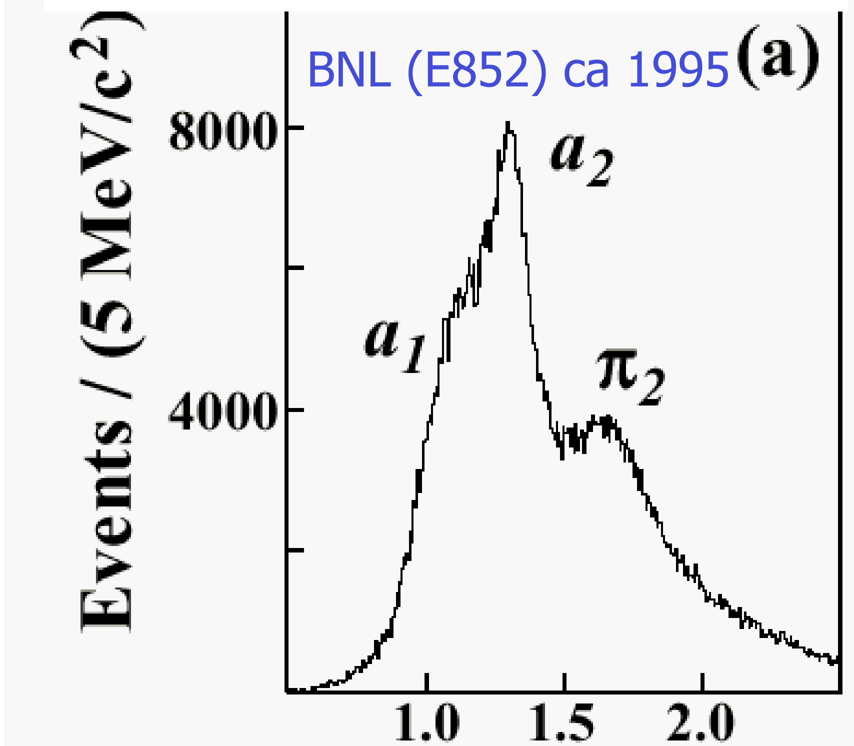

E852 2003
Full sample

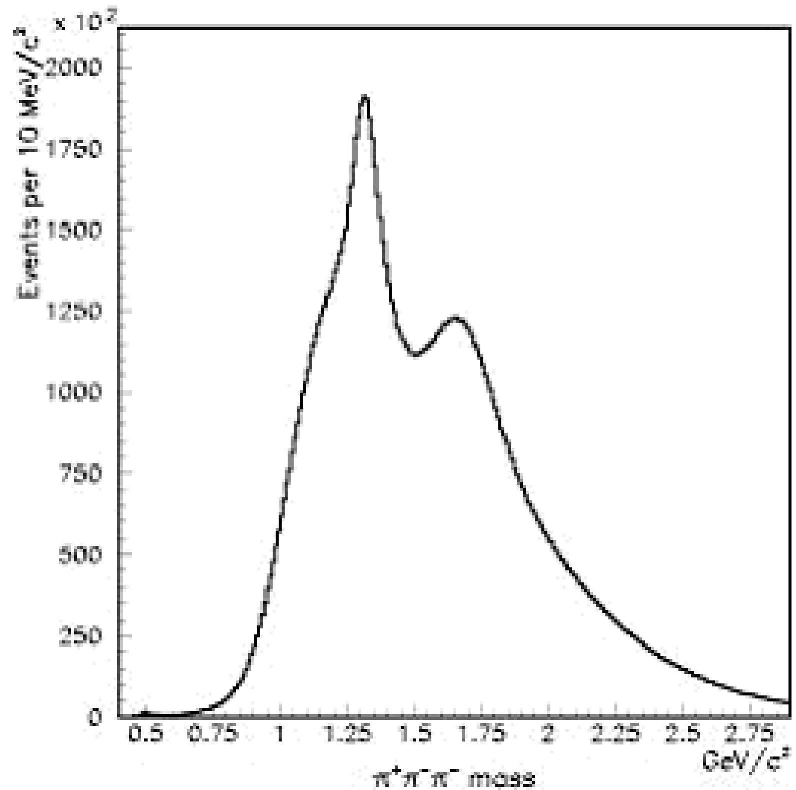

Have we seen exotic mesons

The $\pi_1(1600)$ story in $\pi^+\pi^-\pi^-$

Correlation of Phase & Intensity

1^{-+}

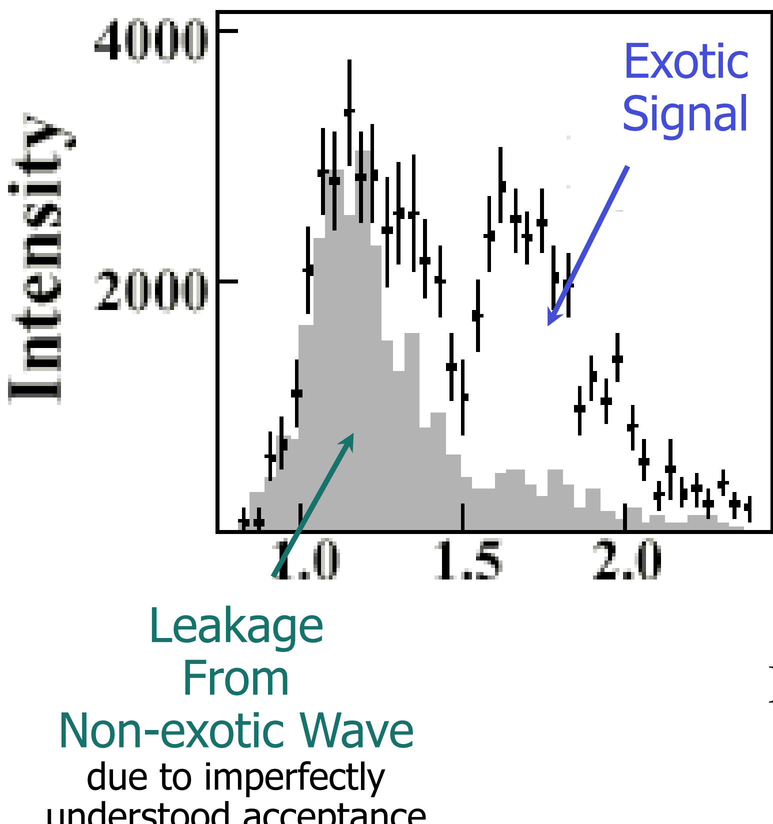

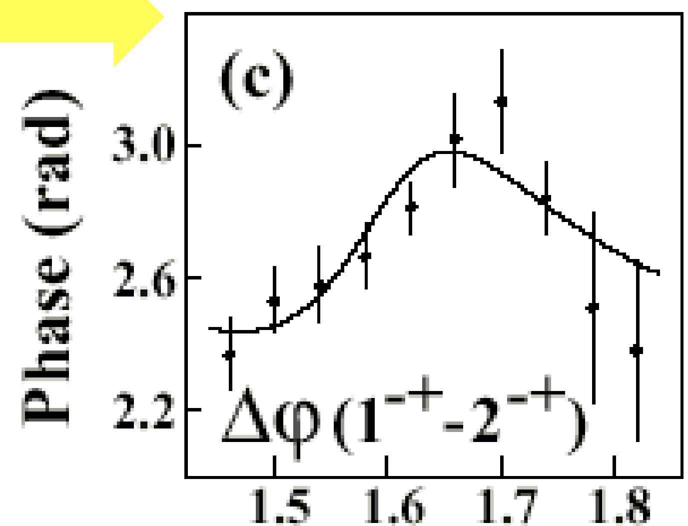

$M(\pi^+\pi^-\pi^-)\ \left[\mathrm{GeV}/c^2\right]$

Based on 250K events   Full sample = 3M + 2M events!

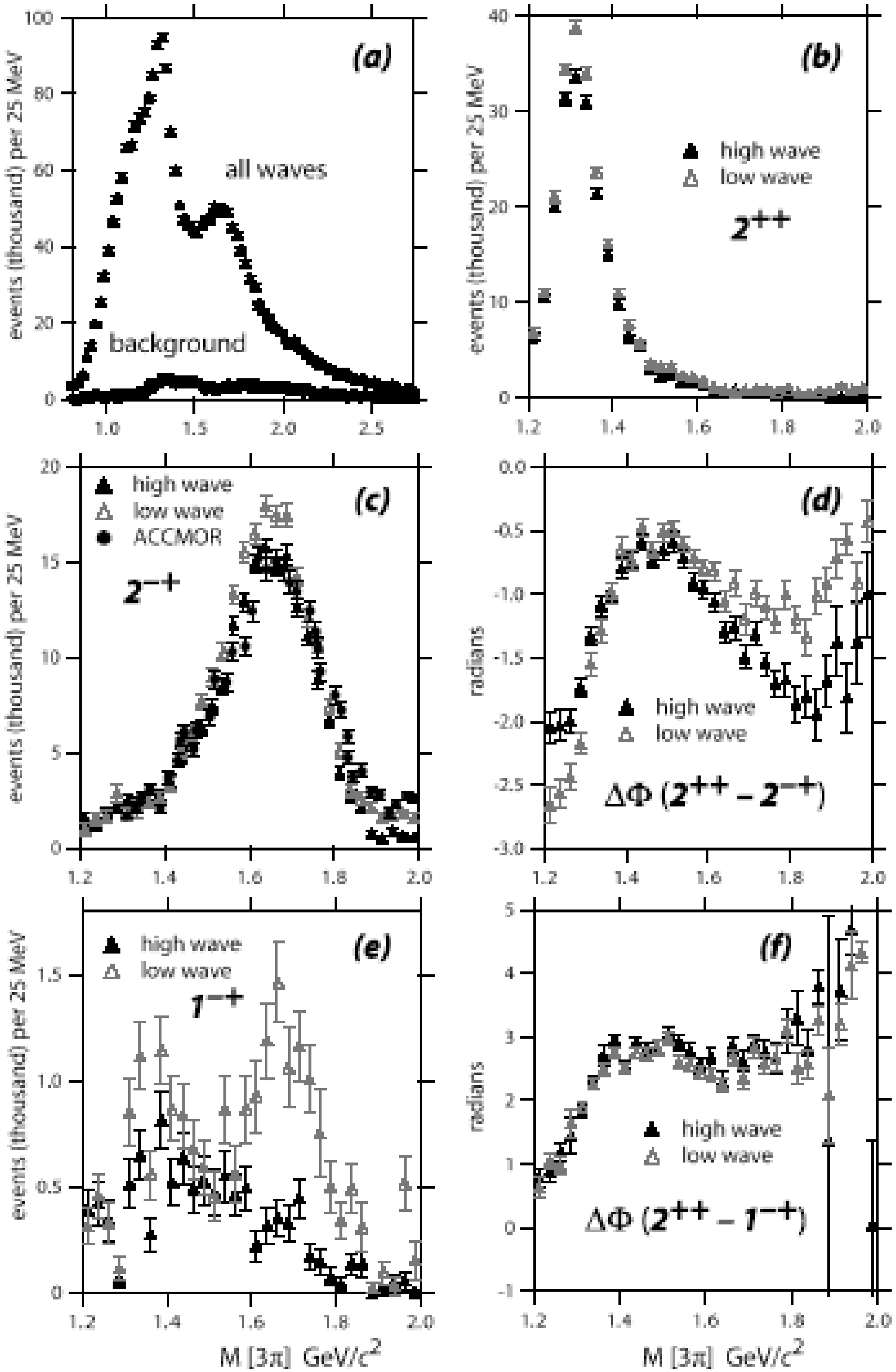

(a)
all waves
background
events (thousand) per 25 MeV
(b)
high wave
low wave
2++
(c)
high wave
low wave
ACCMOR
2−+
(d)
high wave
low wave
ΔΦ (2++ − 2−+)
radians
(e)
high wave
low wave
1−+
(f)
high wave
low wave
ΔΦ (2++ − 1−+)
M [3π] GeV/c2

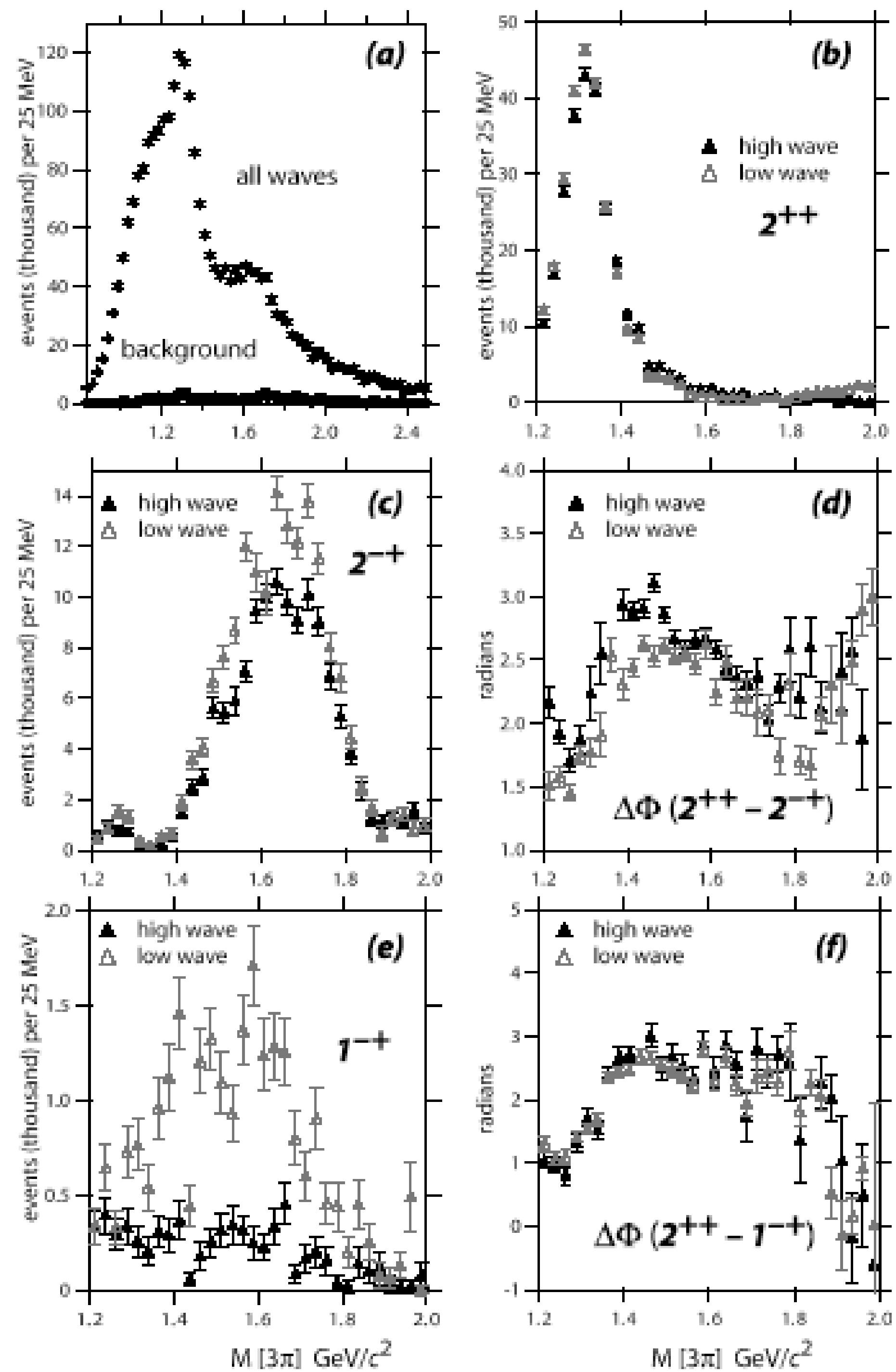

(a)
all waves
background
events (thousand) per 25 MeV
(b)
high wave
low wave
2++
(c)
high wave
low wave
2−+
(d)
high wave
low wave
ΔΦ (2++ − 2−+)
radians
(e)
high wave
low wave
1−+
(f)
high wave
low wave
ΔΦ (2++ − 1−+)
M [3π] GeV/c2

How to generate an exotic

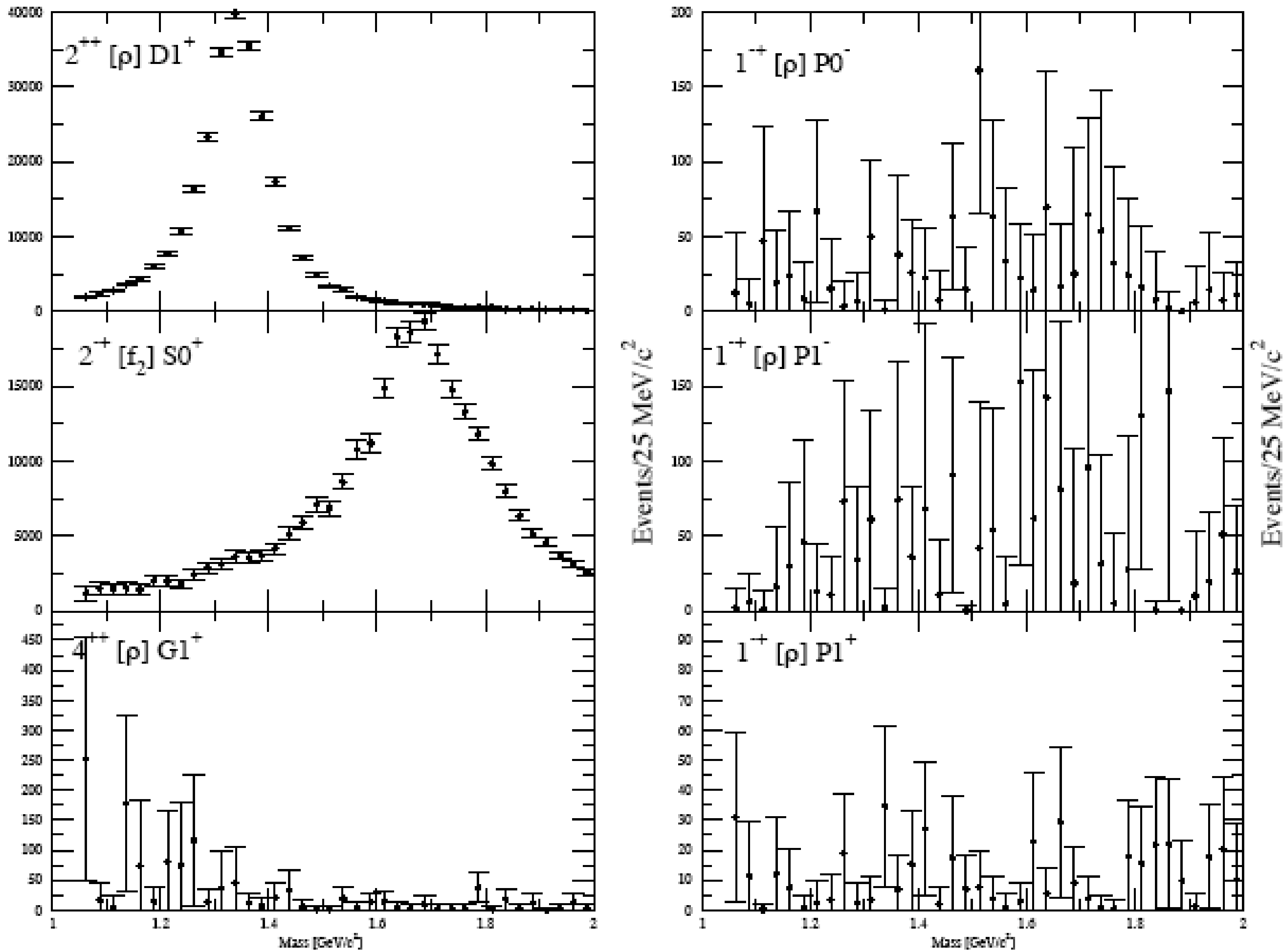

Figure 1. PWA with acceptance correction. The only waves which have non-zero intensity are those that were used to generate artificial data sample. There are no signs of the leakage.

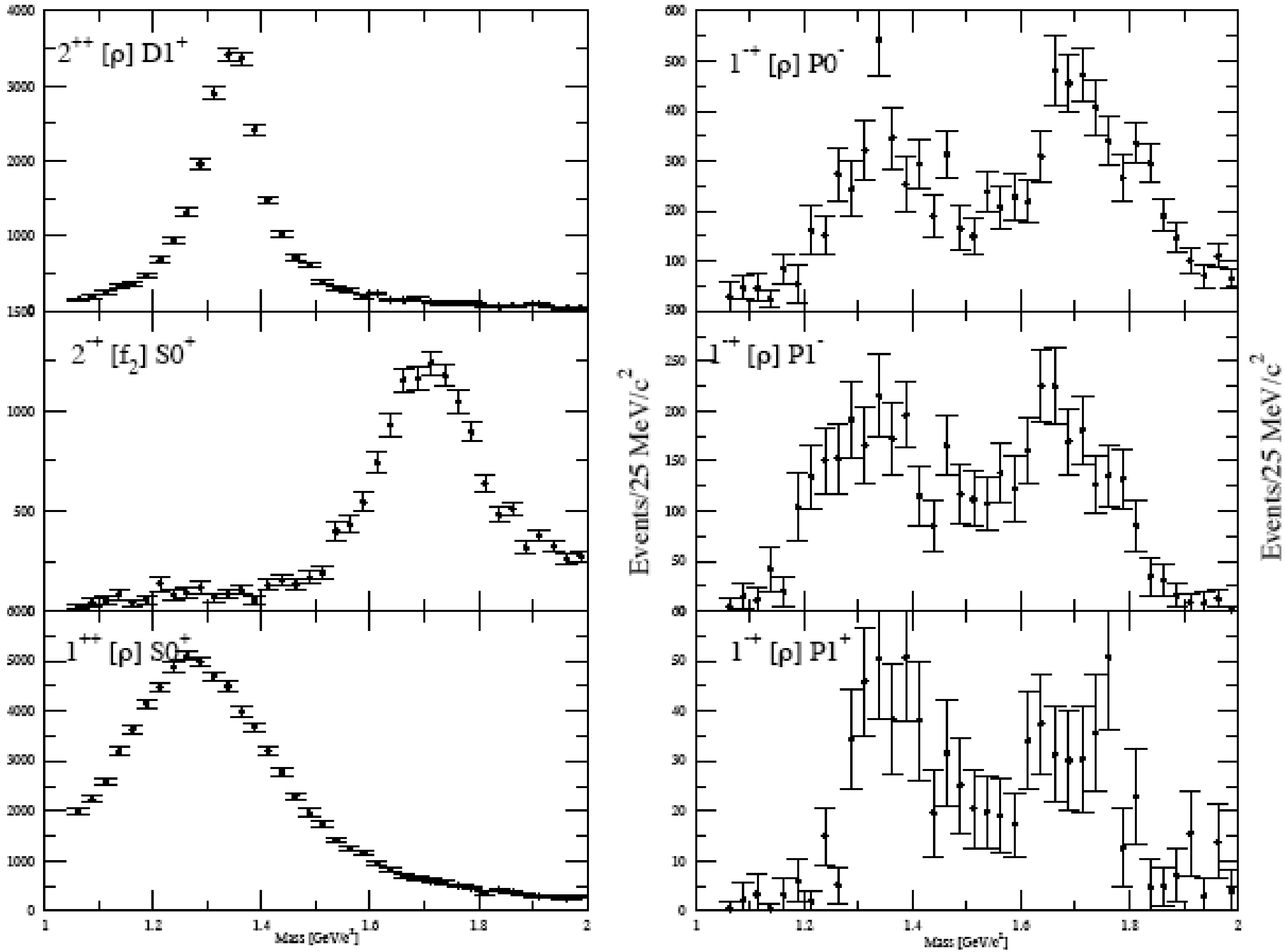

Figure 5. PWA on artificial data sample without acceptance correction and with insufficient number of waves. Notice how leakage shows up in all exotic waves.

Now onto the 5q

5q: positive results

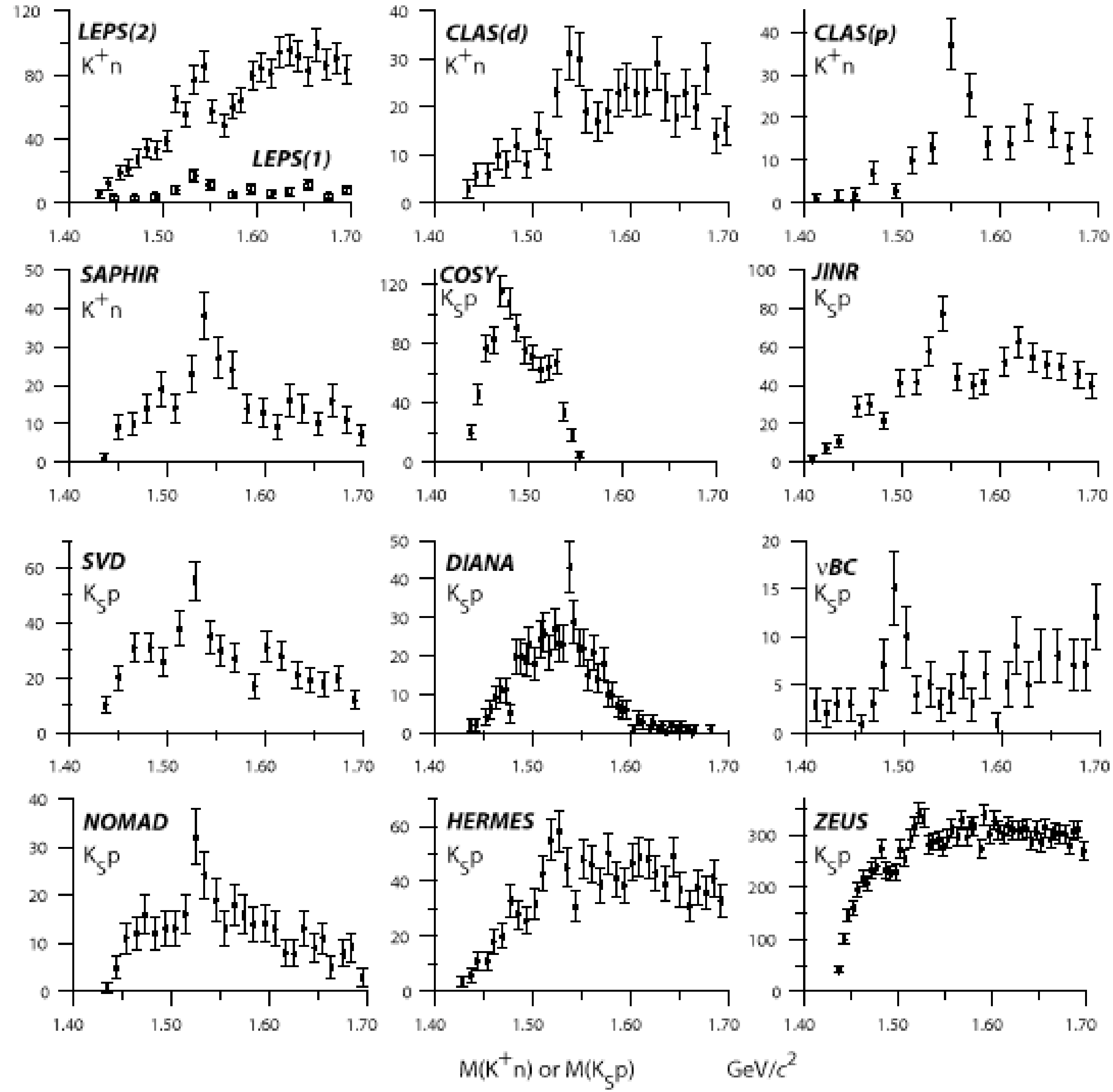

Table 1. Positive signals for pentaquark states. Please see the text regarding the final state neutron in the LEPS, CLAS and SAPHIR experiments.

Experiment	Reaction	State	Mode	Reference
LEPS(1)	$\gamma C_{12} \to K^+K^-X$	θ^+	K^+n	[4]
LEPS(2)	$\gamma d \to K^+K^-X$	θ^+	K^+n	[5]
CLAS(d)	$\gamma d \to K^+K^-(n)p$	θ^+	K^+n	[6]
CLAS(p)	$\gamma p \to K^+K^-\pi^+(n)$	θ^+	K^+n	[7]
SAPHIR	$\gamma p \to K^0_S K^+(n)$	θ^+	K^+n	[8]
COSY	$pp \to \Sigma^+ K^0_S p$	θ^+	$K^0_S p$	[9]
JINR	$p(C_3H_8) \to K^0_S pX$	θ^+	$K^0_S p$	[10]
SVD	$pA \to K^0_S pX$	θ^+	$K^0_S p$	[11]
DIANA	$K^+Xe \to K^0_S p(Xe)'$	θ^+	$K^0_S p$	[12]
νBC	$\nu A \to K^0_S pX$	θ^+	$K^0_S p$	[13]
NOMAD	$\nu A \to K^0_S pX$	θ^+	$K^0_S p$	[14]
HERMES	quasi-real photoproduction	θ^+	$K^0_S p$	[15]
ZEUS	$ep \to K^0_S pX$	θ^+	$K^0_S p$	[16]
NA49	$pp \to \Xi\pi X$	Ξ_5	$\Xi\pi$	[17]
H1	$ep \to (D^*p)X$	θ_c	D^*p	[18]

Dzierba, Meyer, AS

5q: negative results

Table 2. Recent negative searches for pentaquark states. For each pentaquark state (P) we indicated with a $-$ that the state was not included in the search while $\Downarrow$ indicates that the state was searched for and not observed and $\Uparrow$ indicates that the state was searched for and observed.

Experiment	Search Reaction	θ^+	Ξ_5	θ_c	Reference
ALEPH	Hadronic Z decays	$\Downarrow$	$\Downarrow$	$\Downarrow$	[19]
BaBar	$e^+e^- \to \Upsilon(4S)$	$\Downarrow$	$\Downarrow$	$-$	[20]
BELLE	$KN \to PX$	$\Downarrow$	$-$	$\Downarrow$	[21]
BES	$e^+e^- \to J/\psi(\psi(2S) \to \theta\bar{\theta}$	$\Downarrow$	$-$	$\Downarrow$	[22]
CDF	$p\bar{p} \to PX$	$\Downarrow$	$\Downarrow$	$\Downarrow$	[23]
COMPASS	$\mu^+(^6LiD) \to PX$	$\Downarrow$	$\Downarrow$	$-$	[24]
DELPHI	Hadronic Z decays	$\Downarrow$	$-$	$-$	[25]
E690	$pp \to PX$	$\Downarrow$	$\Downarrow$	$-$	[26]
FOCUS	$\gamma p \to PX$	$\Downarrow$	$\Downarrow$	$\Downarrow$	[27]
HERA-B	$pA \to PX$	$\Downarrow$	$\Downarrow$	$-$	[28]
HyperCP	$(\pi^+, K^+, p)Cu \to PX$	$\Downarrow$	$-$	$-$	[29]
LASS	$K^+p \to K^+n\pi^+$	$\Downarrow$	$-$	$-$	[30]
L3	$\gamma\gamma \to \theta\bar{\theta}$	$\Downarrow$	$-$	$-$	[25, 31]
PHENIX	$AuAu \to PX$	$\Downarrow$	$-$	$-$	[32]
SELEX	$(\pi, p, \Sigma)p \to PX$	$\Downarrow$	$-$	$-$	[33]
SPHINX	$pC(N) \to \theta^+C(N)$	$\Downarrow$	$-$	$-$	[34]
WA89	$\Sigma^-N \to PX$	$-$	$\Downarrow$	$-$	[36]
ZEUS	$ep \to PX$	$\Uparrow$	$\Downarrow$	$\Downarrow$	[16, 37, 38]

Table 3. A tabulation of statistics for the observations of the θ^+. See text for descriptions of the statistical significance as quoted in the three columns of ratios. The column labeled Published is the significance quoted in the publication.

Experiment	Signal s	Background b	Significance Published	$\frac{s}{\sqrt{b}}$	$\frac{s}{\sqrt{s+b}}$	$\frac{s}{\sqrt{s+2b}}$
LEPS(1) [4]	19	17	4.6	4.6	3.2	2.6
LEPS(2) [5]	56	162		4.4	3.8	2.9
CLAS(d) [6]	43	54	5.2	5.9	4.4	3.5
CLAS(p) [7]	41	35	7.8	6.9	4.7	3.9
SAPHIR [8]	55	56	4.8	7.3	5.2	4.3
COSY [9]	57	95	$4-6$	5.9	4.7	3.7
JINR [10]	88	192	5.5	6.4	5.3	4.1
SVD [11]	35	93	5.6	3.6	3.1	2.4
DIANA [12]	29	44	4.4	4.4	3.4	2.7
νBC [13]	18	9	6.7	6.0	3.5	3.0
NOMAD [14]	33	59	4.3	4.3	3.4	2.7
HERMES [15]	51	150	$4.3-6.2$	4.2	3.6	2.7
ZEUS [16]	230	1080	4.6	7.0	6.4	4.7

Kinematic reflections

3 body kinematics

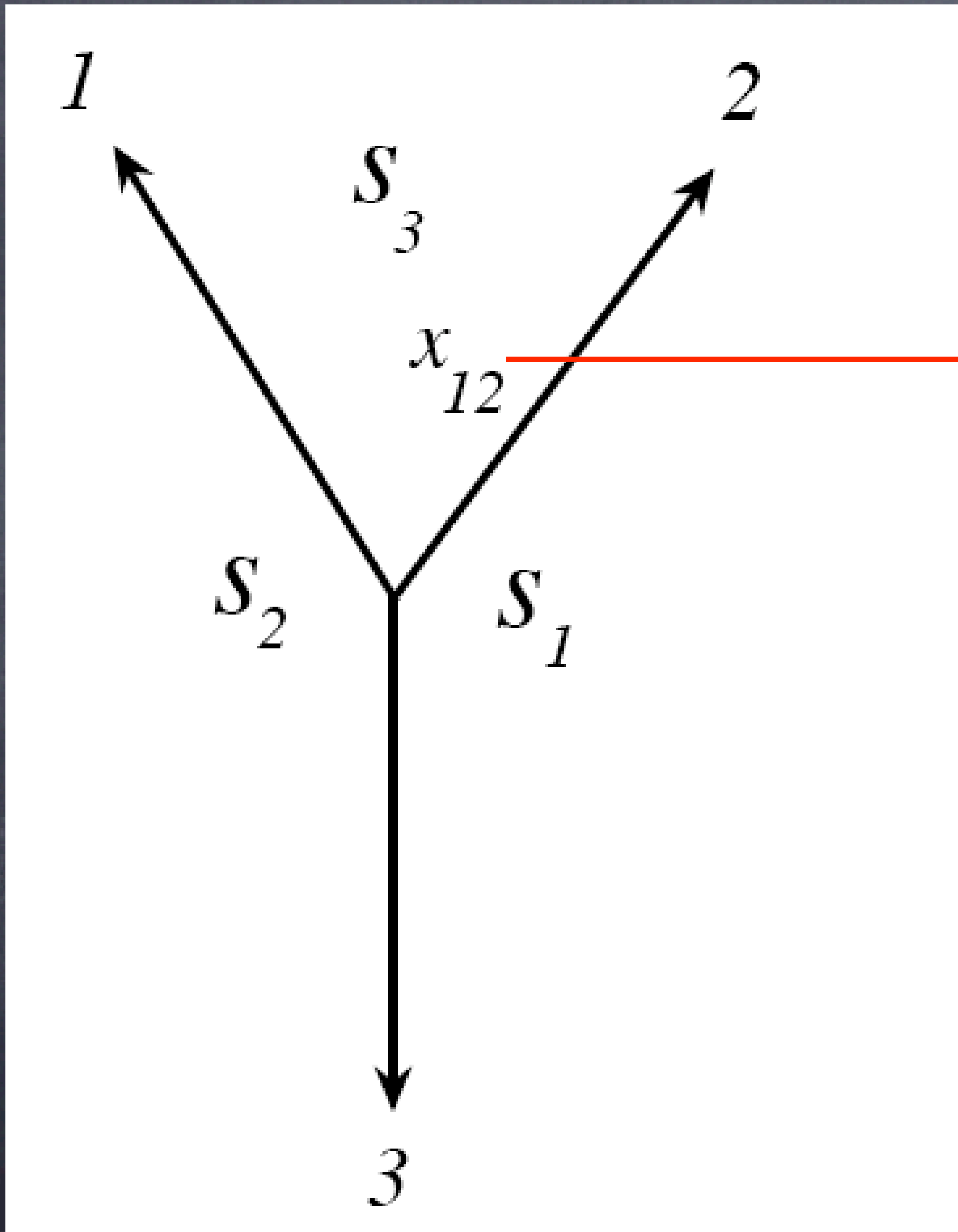

$$s_1 + s_2 + s_3 = s - m_1^2 - m_2^2 - m_3^2$$

cos of the helicity angle of 1 in the (12) rest frame

$$s_2 = s_2(s_1, s, x_{12})$$

3-particle Dalitz plot

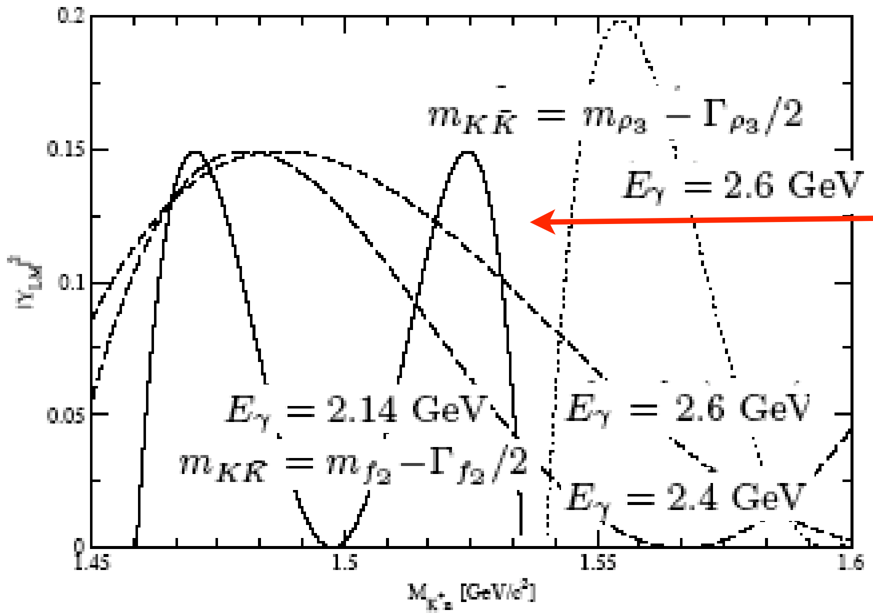

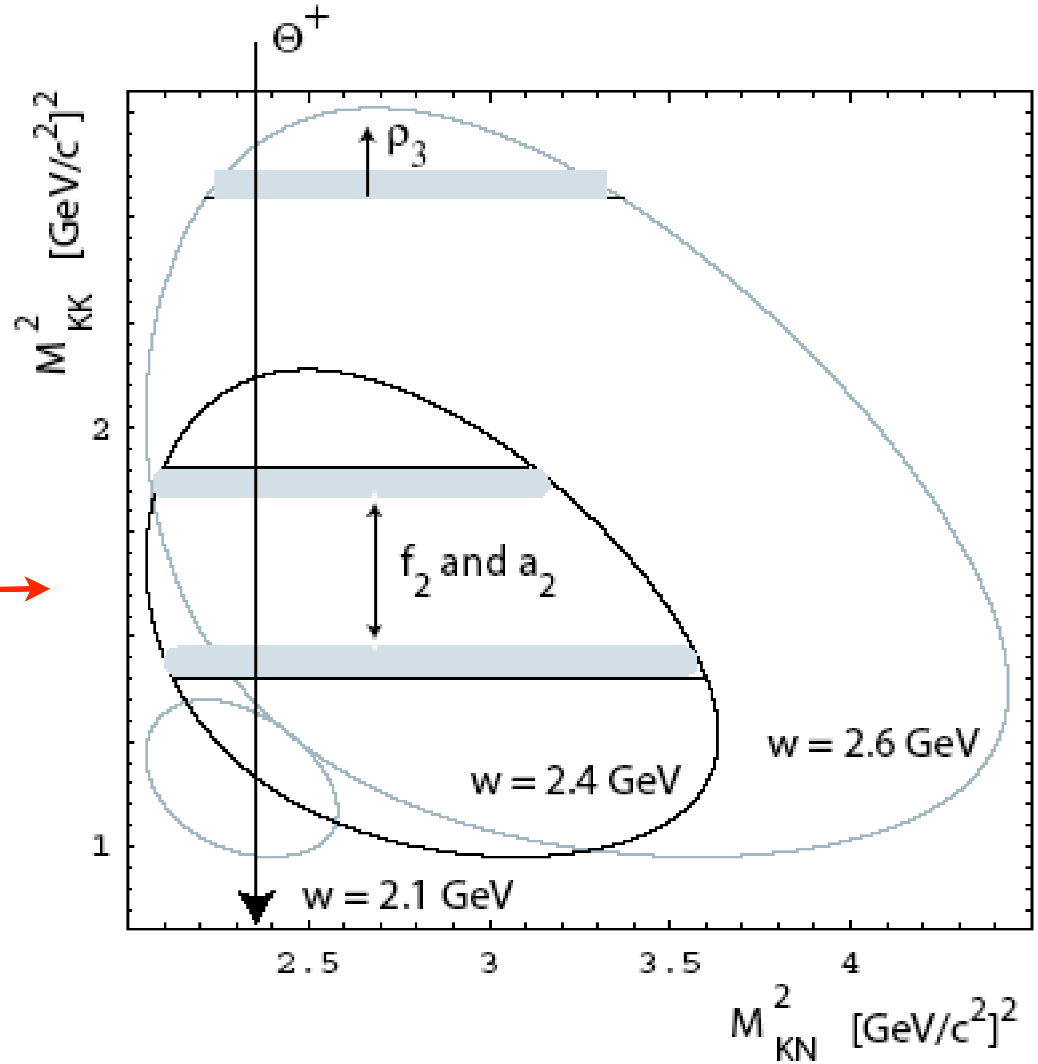

FIG. 1: Boundaries of the m^2_{KK} versus m^2_{KN} Dalitz plot for three different values of w, the energy available to the $K\bar{K}N$ system, 2.1, 2.4 and 2.6 GeV. For the data of ref. [2], the observed distribution in w rises from 2.1 GeV, peaks at 2.4 and falls to zero near 2.6 GeV. Horizontal lines denote the region spanned by the f_2 and a_2 mesons defined by their half-widths and the region of the ρ_3 starting with its central mass less its half-width. The vertical line denotes the square of the Θ mass.

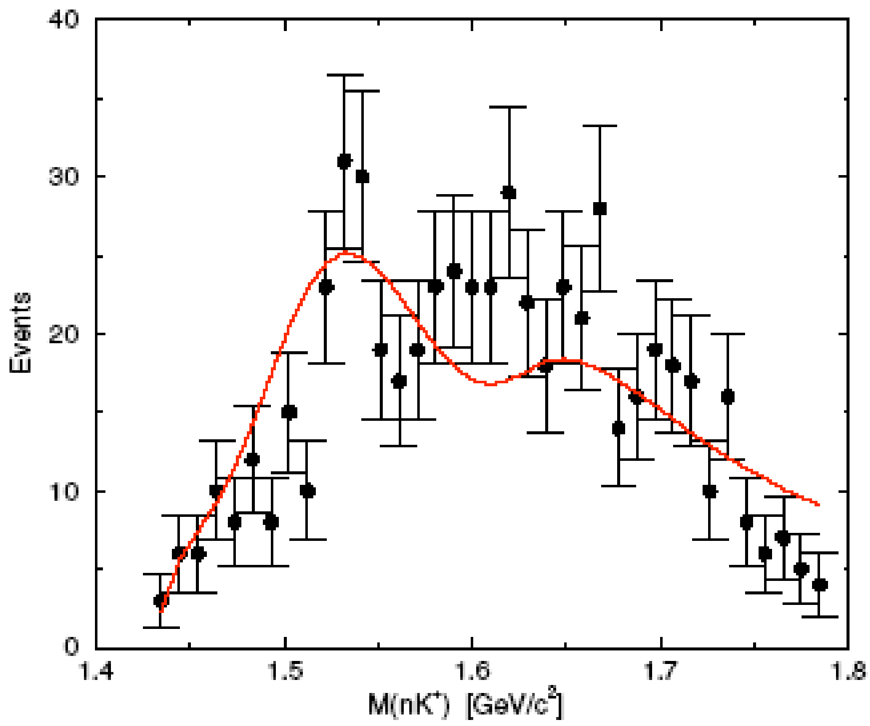

FIG. 3: The calculated (solid line) m_{KN} distribution, as described in the text, compared with the data from [2]

Reaction	Beam energy GeV	Cross Section μb	Ref
$\gamma p \to f_2 p$	2.3-2.6	1.3 ± 0.37	[6]
$\gamma p \to f_2 p$	2.6-3.25	0.39 ± 0.13	[6]
$\gamma p \to f_2 p$	3.25-4.0	0.19 ± 0.06	[6]
$\gamma p \to f_2 p$	4.0-6.3	0.1 ± 0.1	[6]
$\gamma p \to a_2^+ n$	4.2 ± 0.5	1.14 ± 0.43	[7]
$\gamma p \to a_2^+ n$	5.25 ± 0.55	0.85 ± 0.43	[7]
$\gamma p \to a_2^+ n$	7.5 ± 0.7	0.43 ± 0.43	[7]
$\gamma p \to K^+K^- p$	2.8	1.0 ± 0.1	[8]
$\gamma p \to K^+K^- p$	4.7	0.7 ± 0.1	[8]

TABLE I: Photoproduction cross sections for the $f_2(1275)$ and $a_2(1320)$ resonances and the K^+K^- final state.

Physical background has structure >> reduces the statistical significance of the signal

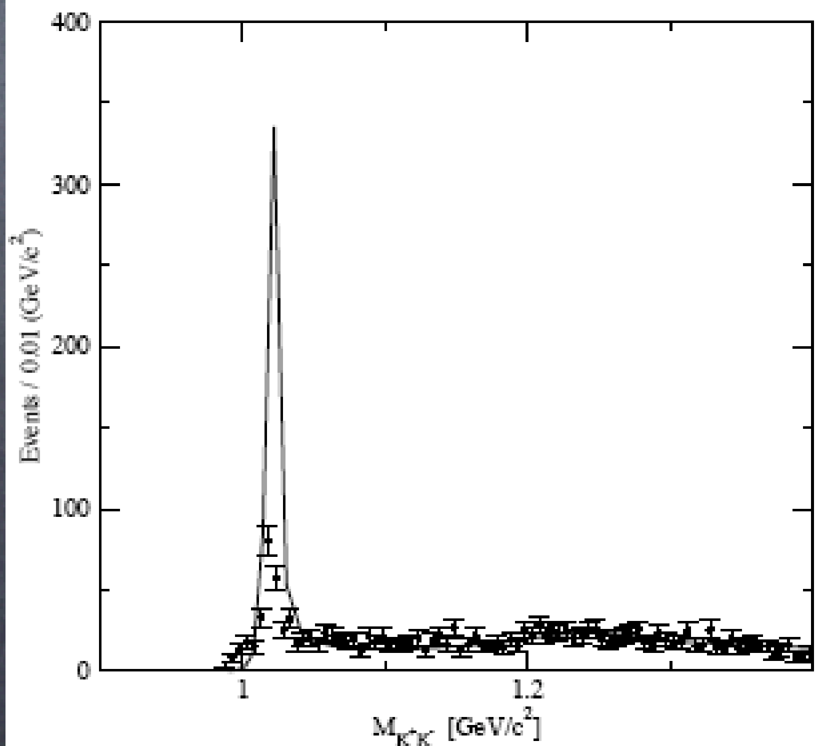

Fake Peaks

Enhancement is broad
- but starting with:

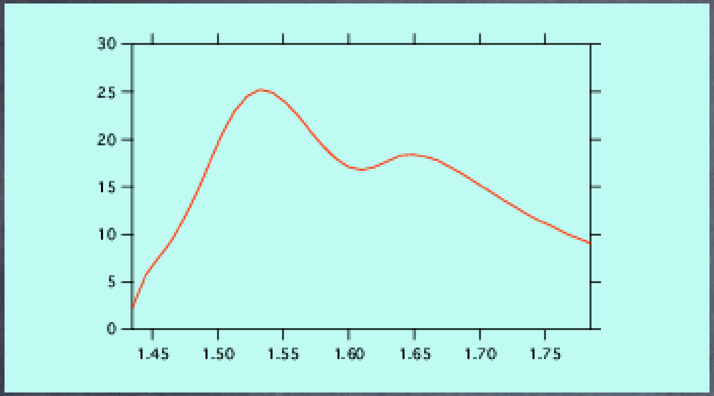

as a parent distribution generate 40 random histograms with 600 events each - 3 of these along with CLAS results appear here

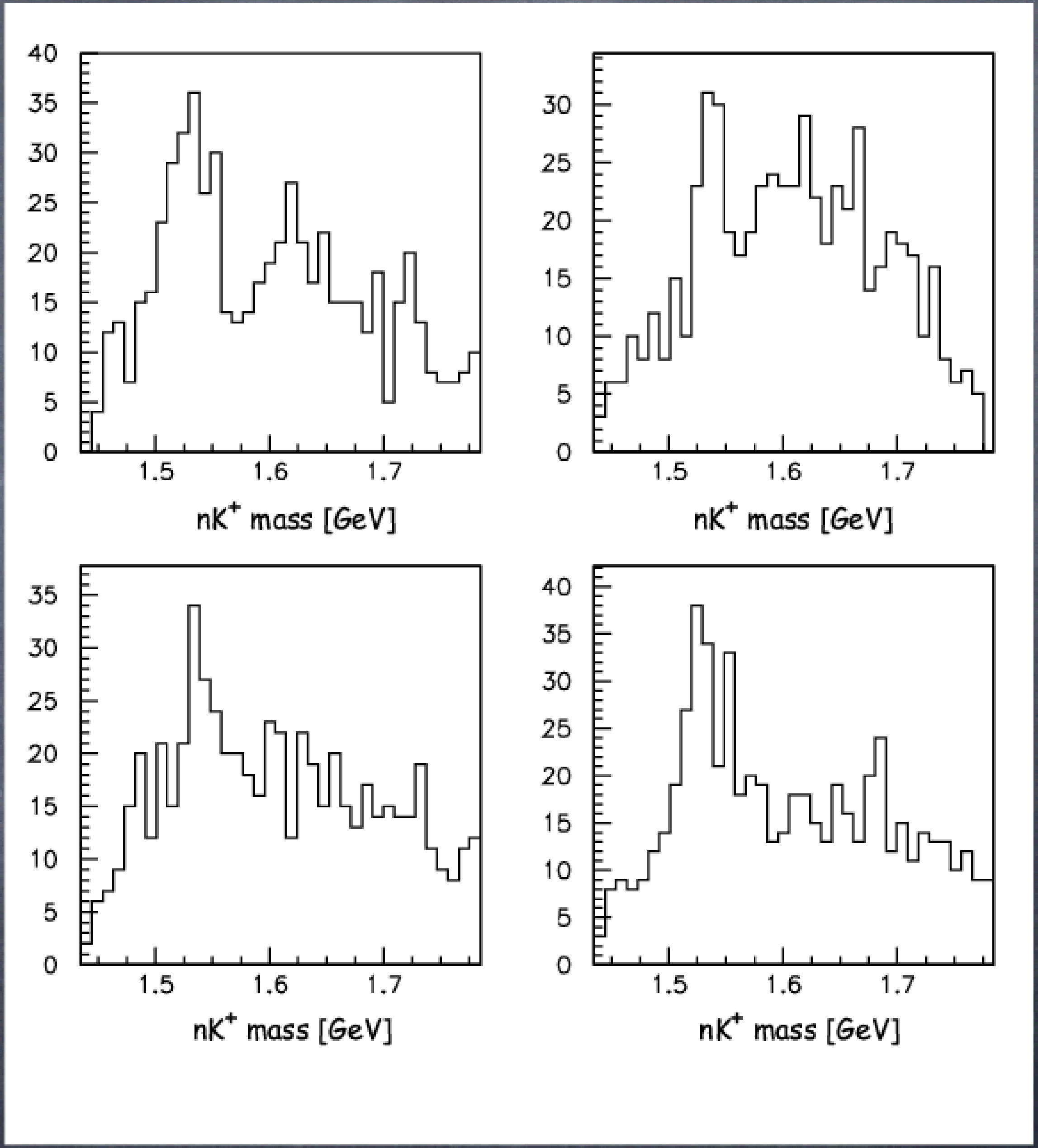

SEARCH FOR THE Z* IN $\pi^- + p \rightarrow K^- + Z^*$ AT 6 AND 8 GeV/c ‡

E. W. ANDERSON, E. J. BLESER‡‡, H. R. BLIEDEN, G. B. COLLINS, D. GARELICK
J. MENES and F. TURKOT
Brookhaven National Laboratory, Upton, New York, USA

$$\pi^- + p \rightarrow B^{*-} + p$$
$$\hookrightarrow K^0 + K^-$$
$$\rightarrow B^{*0} + n$$
$$\hookrightarrow K^+ + K^- \,.$$

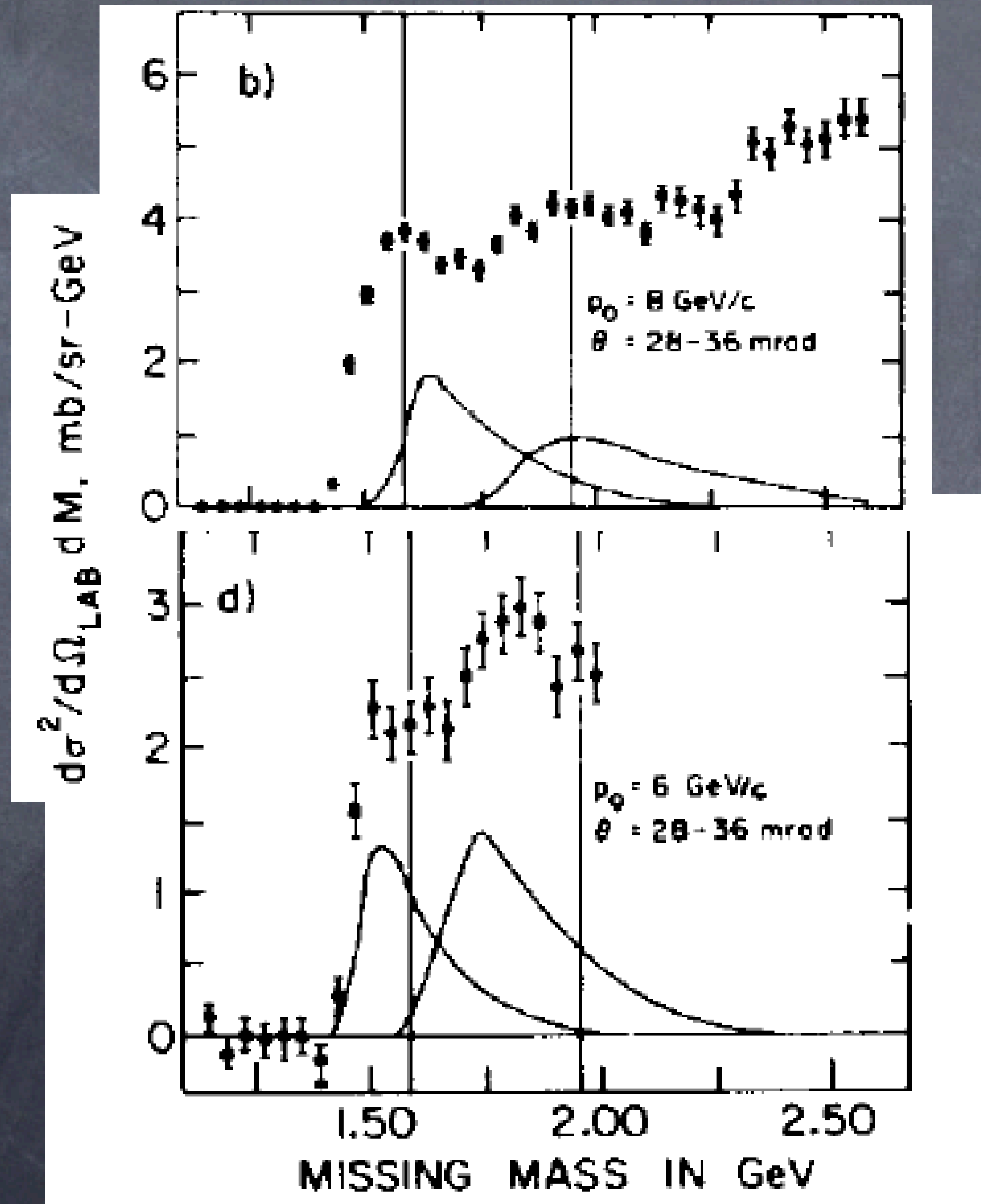

CLAS (proton) $\gamma p \to \pi^+ K^- K^+ n$

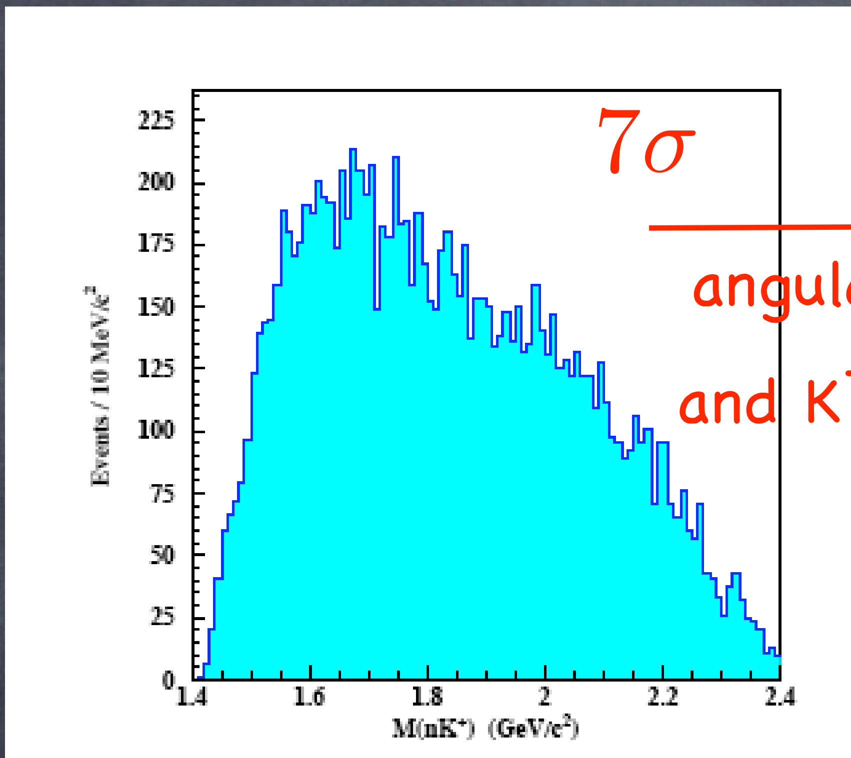

7σ

angular cuts on π^+

and K$^+$ momenta

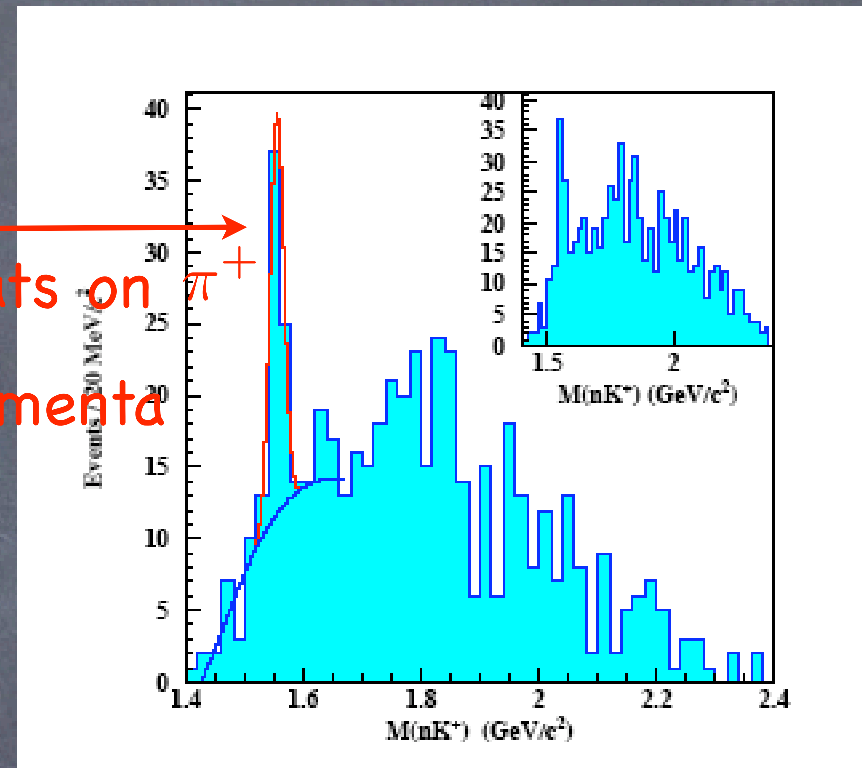

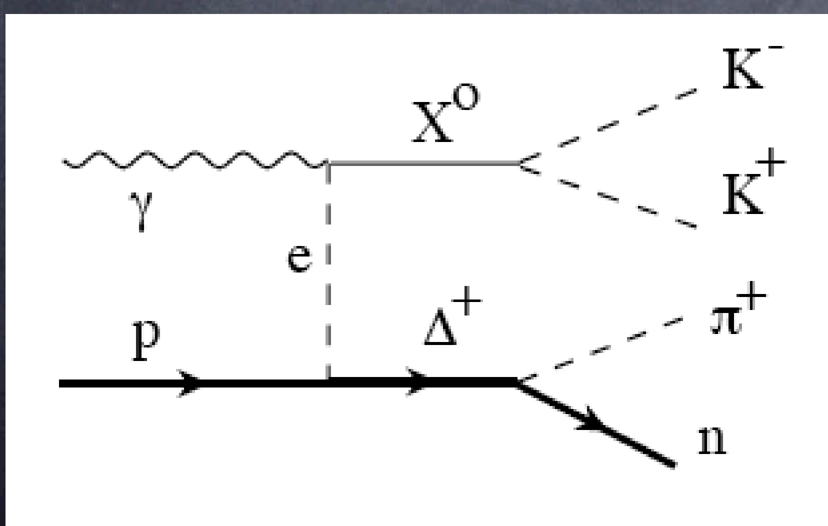

The background and role of cuts have not been studied. Why not associate production of Θ^+ (P.Stoler @ QNP04)

Can generate resonance-like structure in K^+K^-n spectrum and π^+ momentum cut enhances kinematic reflections from decays of K^+K^- resonances

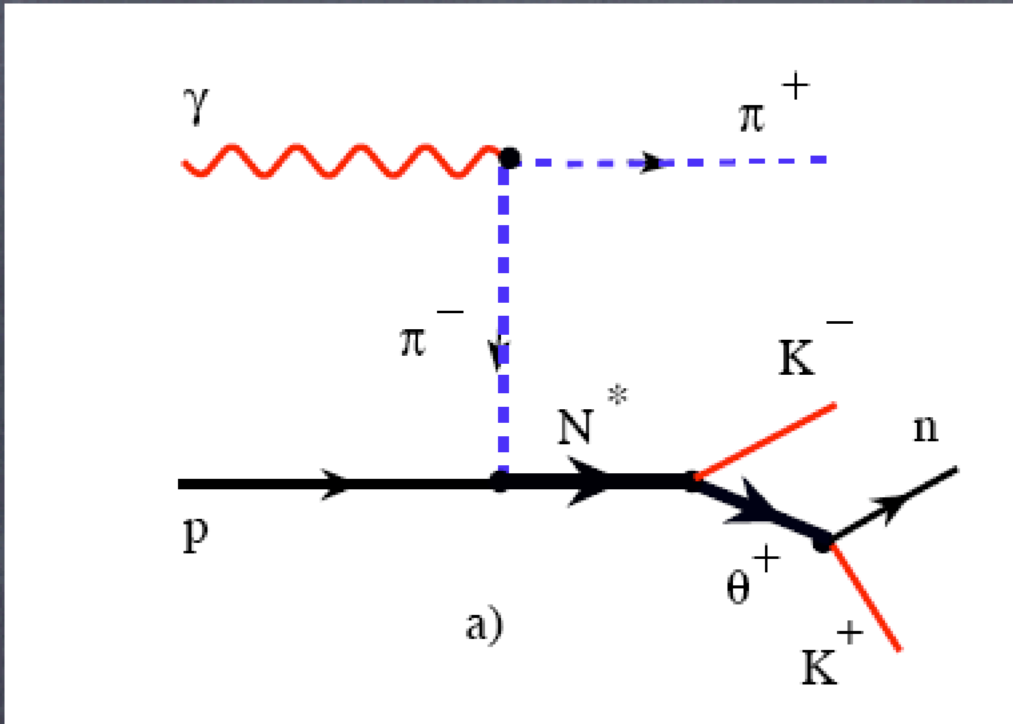

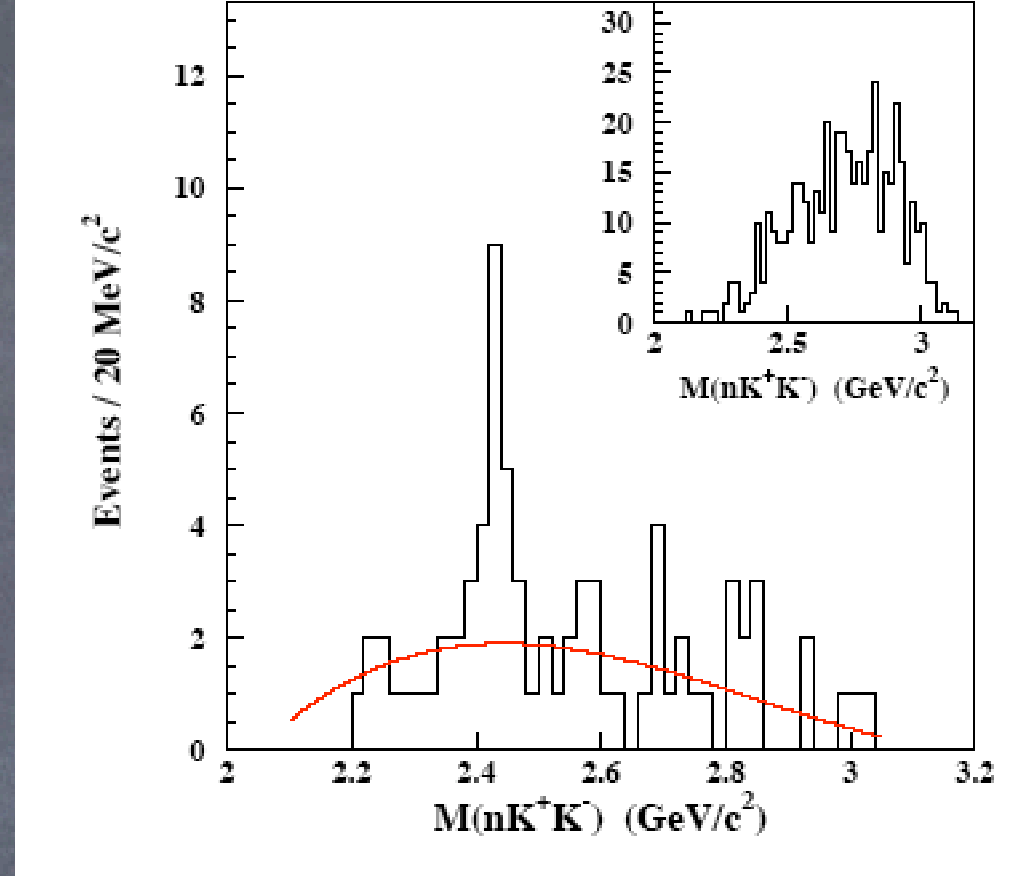

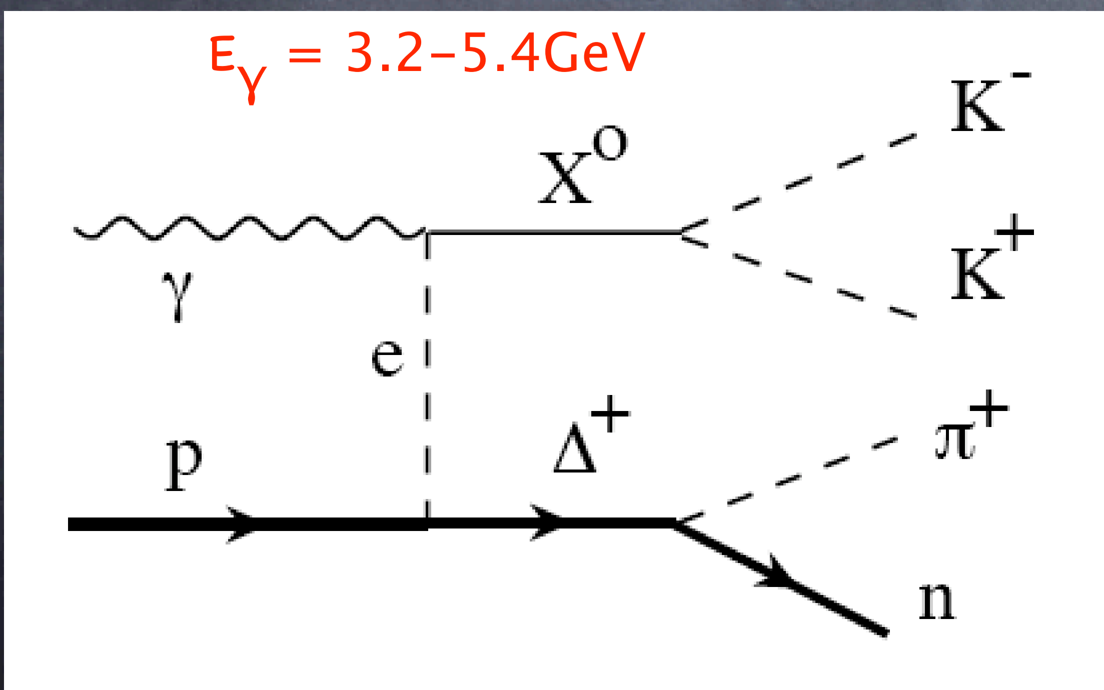

Threshold energies

$X=f_2$ $W=2.51GeV$

$X=a_2$ $W=2.55GeV$

$X=\rho_3$ $W=3.31GeV$

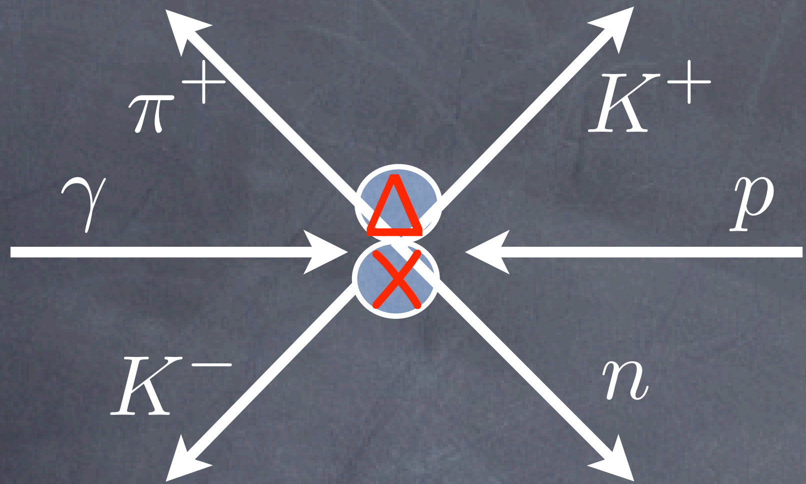

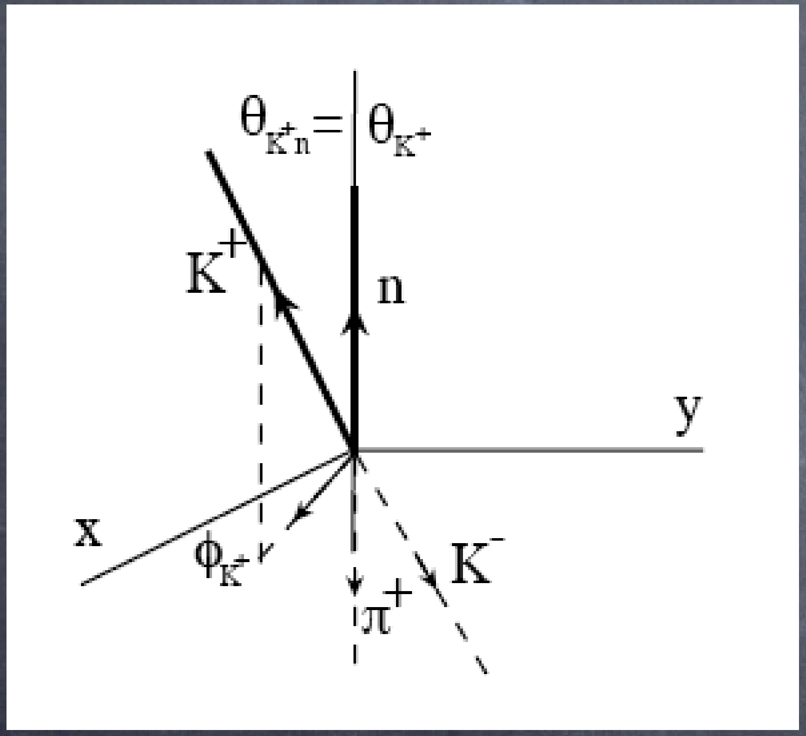

"N*" mass

$$M_{N^*} = 2.23GeV$$

$$M_{N^*} = 2.27GeV$$

$$M_{N^*} = 2.64GeV$$

$$\uparrow$$

$$M_{nK^+K^-} = M_{N^*}$$

is sharp !

$$\cos\theta^*_\pi > 0.8$$

correlates n with K^+ K^- helicity ->possible kinematic reflection

from K^+ K^- resonance

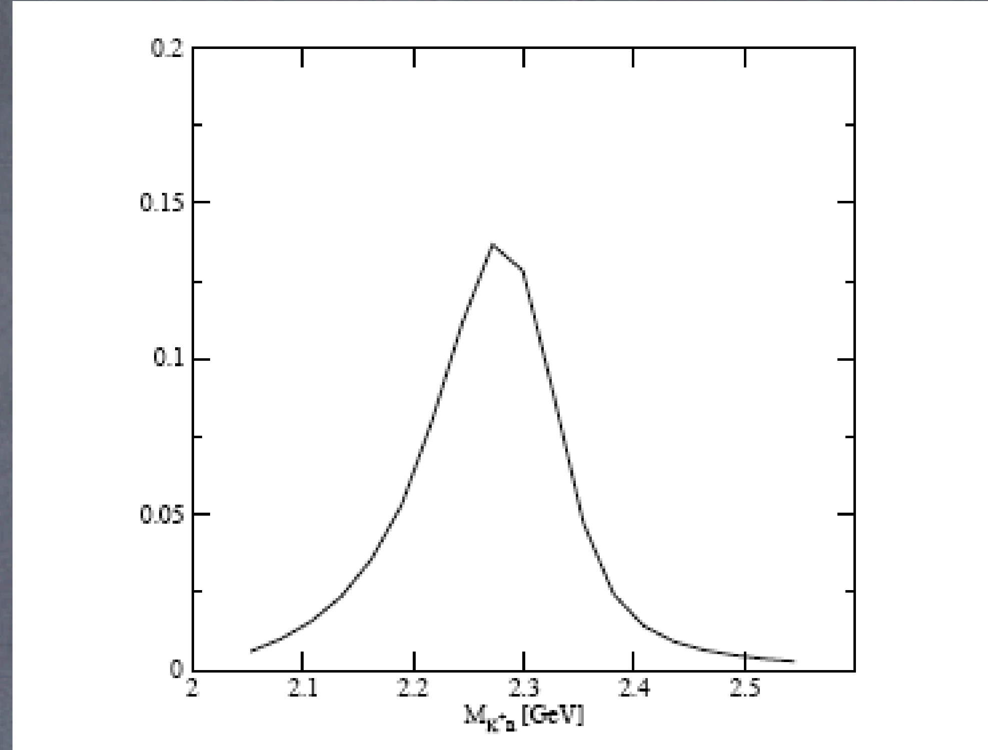

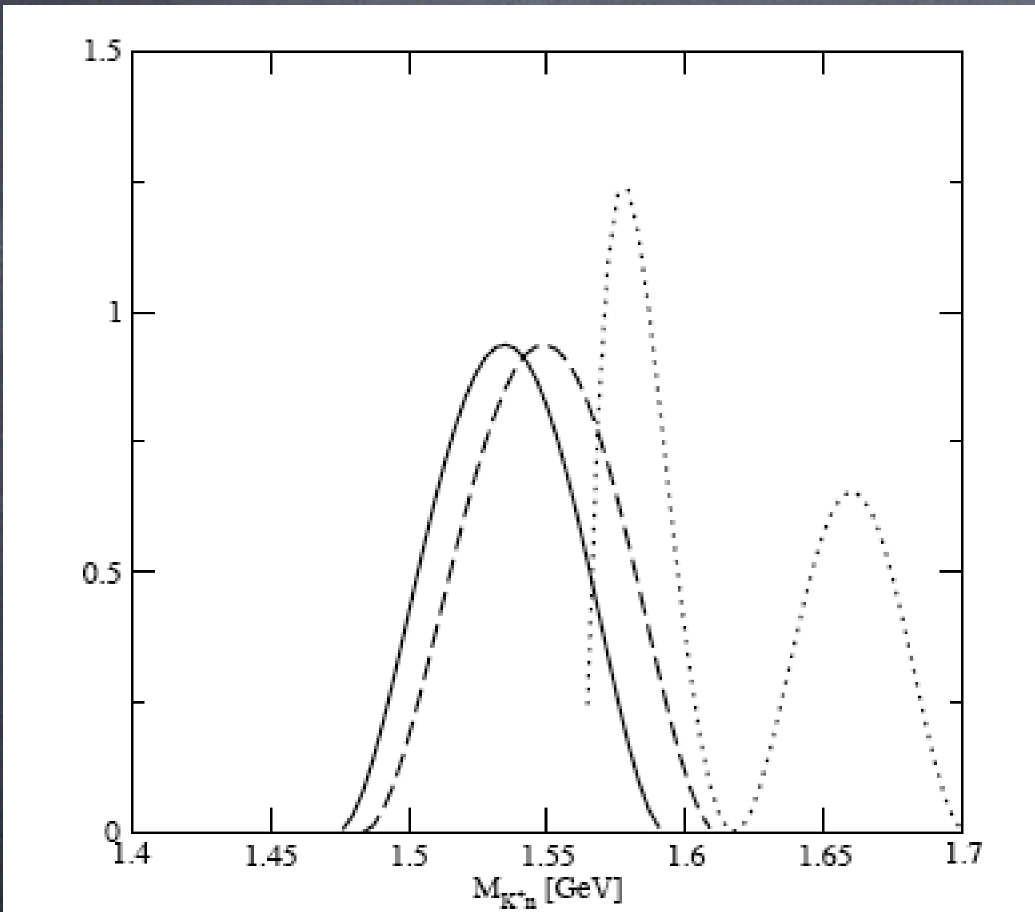

FIG. 3: The nK^+ mass distribution as described by $\int d\phi_{K^+}|Y_{J_X,\lambda_X}(\theta_{K^+n},\phi_{K^+})|^2$, for $\Delta = \Delta(1232)$ and $J_X = \lambda_X = 2$, $X = f_2$, (solid line), $J_X = \lambda_X = 2$, $X = a_2$, (dashed line), and $J_X = 3$, $\lambda_X = 1$, $X = \rho_3$ (dotted line). The $M_{nK^+K^-}$ invariant masses for the three cases are $2.22, 2.27$ and 2.64 GeV, respectively.

DIANA (ITEP, Xe bubble chamber, 850MeV K-beam)

$$K^+ Xe \rightarrow K_s^0 p Xe'$$

no magnetic field

particle identified by their range in Xe

angular cut, p and Ks in the forward direction

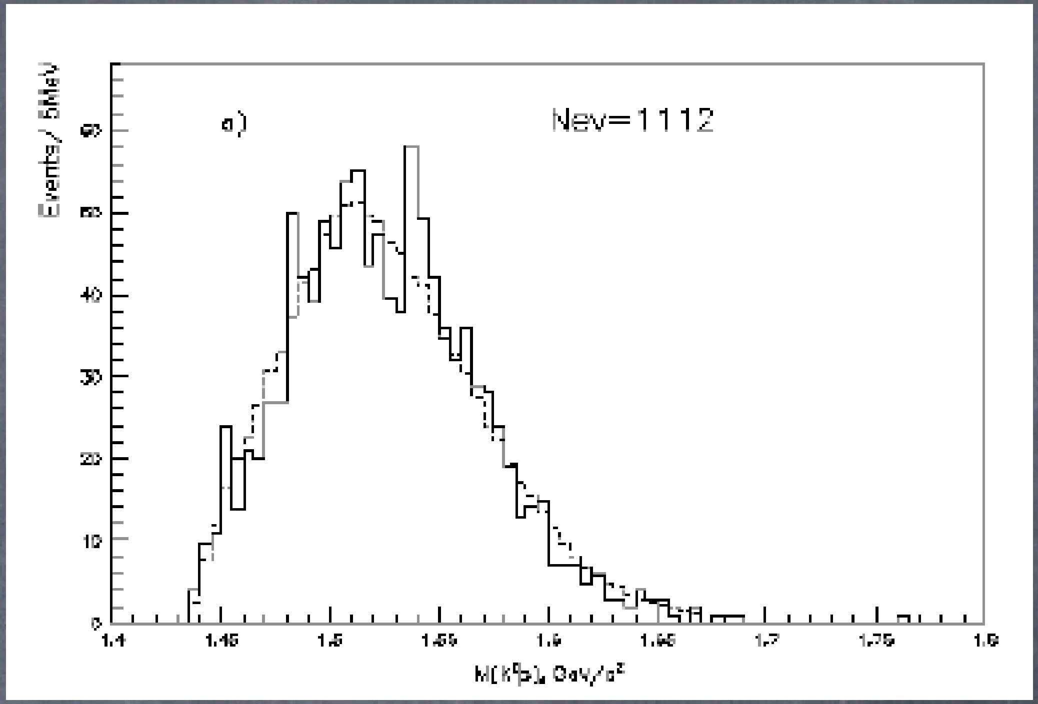

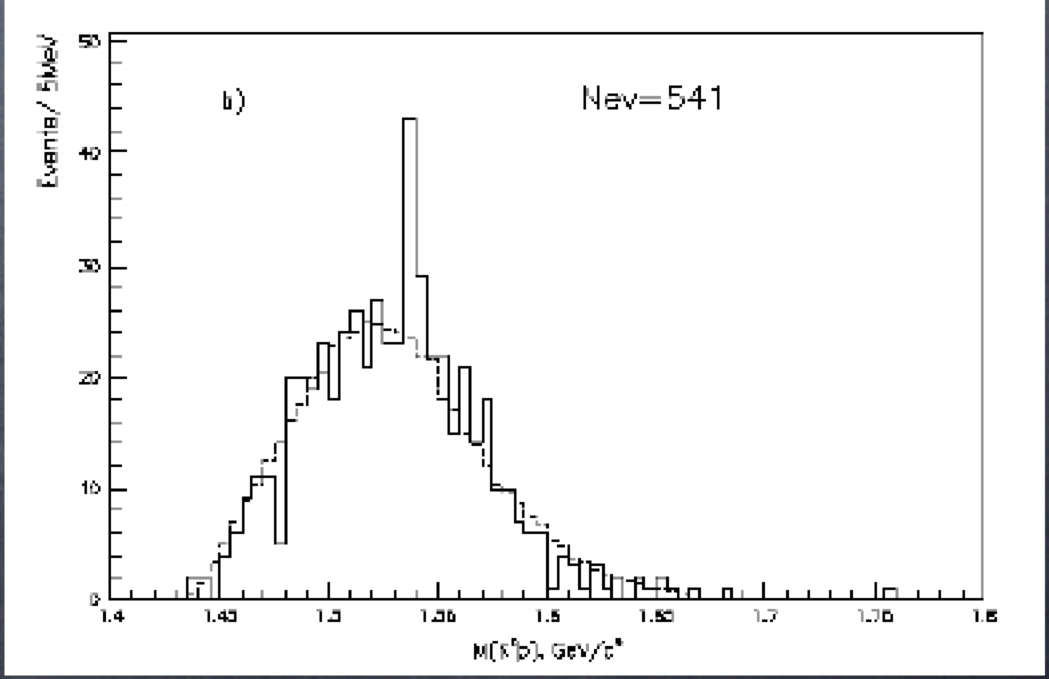

M.Zavertyaev, (hep-ph/0311250)

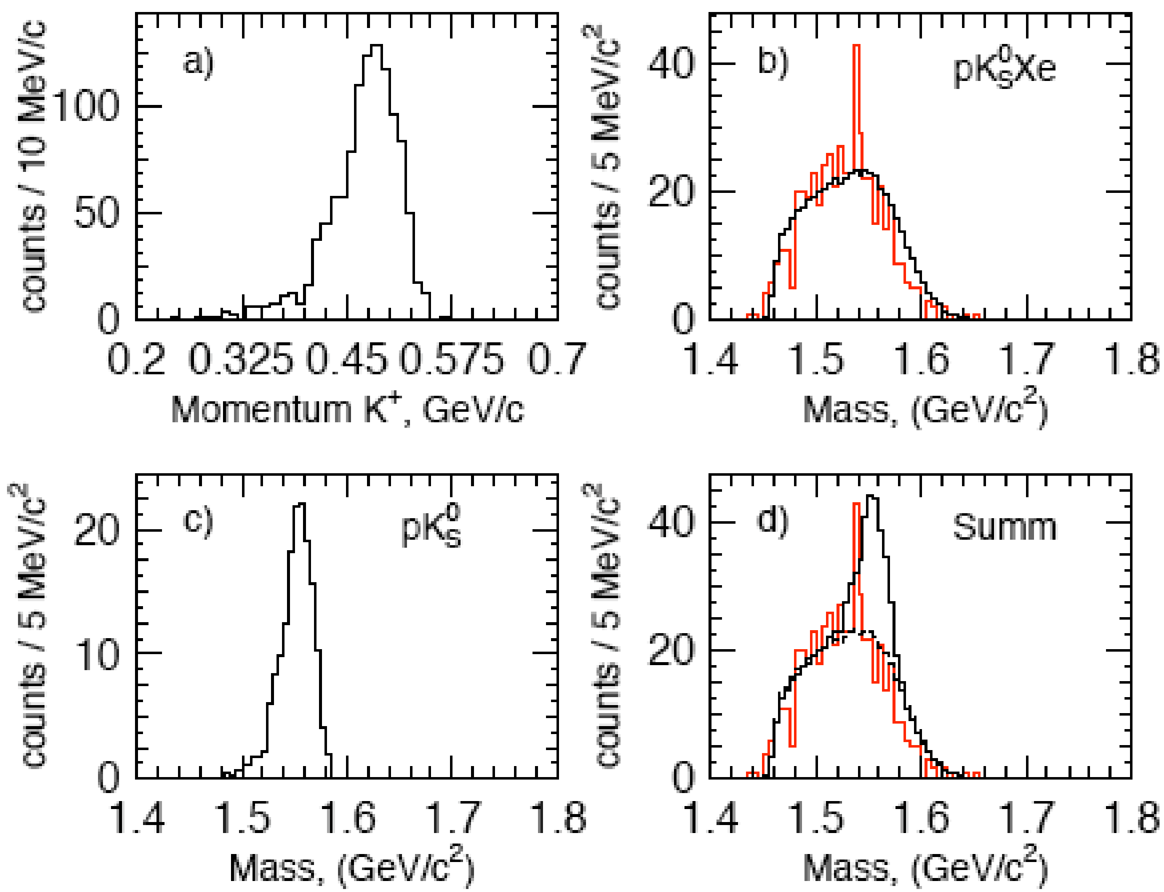

Figure 2: The experimental beam momentum [5] and MC mass spectra distribution corresponding to: b) reaction $K^+Xe \rightarrow K^0_s pXe'$; c) reaction $K^+n \rightarrow K^0_s p$; d) the summ of both b) and c); The histogram in red corresponds to the experimental mass distribution from [5].

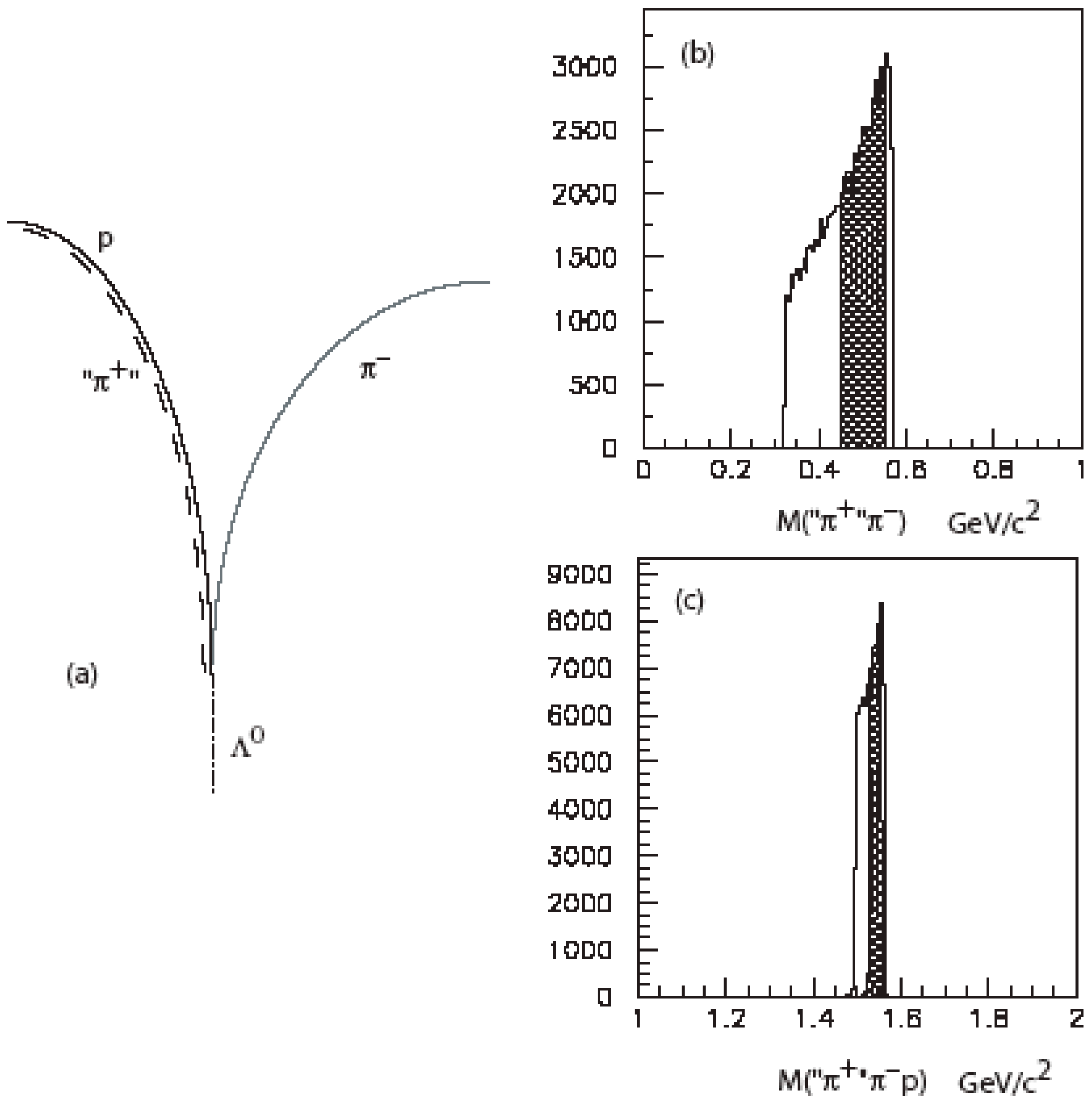

Figure 5. Figure (a) is a schematic of the decay $\Lambda^0(1115) \rightarrow \pi^- p$. The effect of spurious *ghost* tracks from the reconstruction software is considered. In this case a π^+ track is generated. When combined with the π^- from the Λ^0 the effective mass clusters about 0.5 GeV/c^2 as in Figure (b) and when the ghost track is combined with the Λ^0 decay products the effective mass clusters around 1.5 GeV/c^2 as seen in Figure (c). In the shaded distributions the "π^+"π^- mass is required to be near the K_S^0. The mean of the shaded portion of the distribution in Figure (c) is 1.54 GeV/c^2, the mass of the θ^+. In this study the Λ^0 momentum in the LAB frame was uniform from 2 to 100 GeV/c.

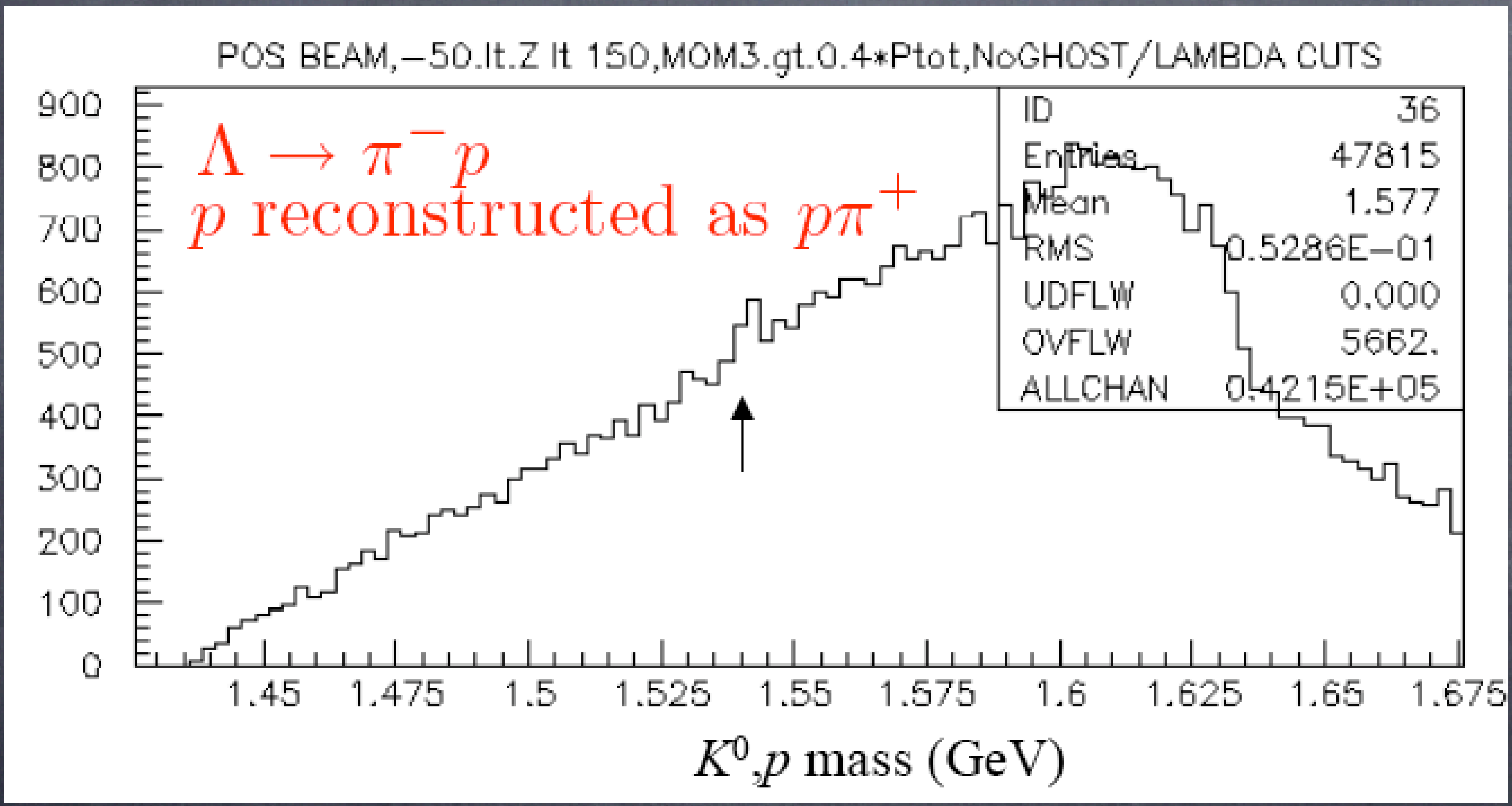

Hyper CP @ FNAL

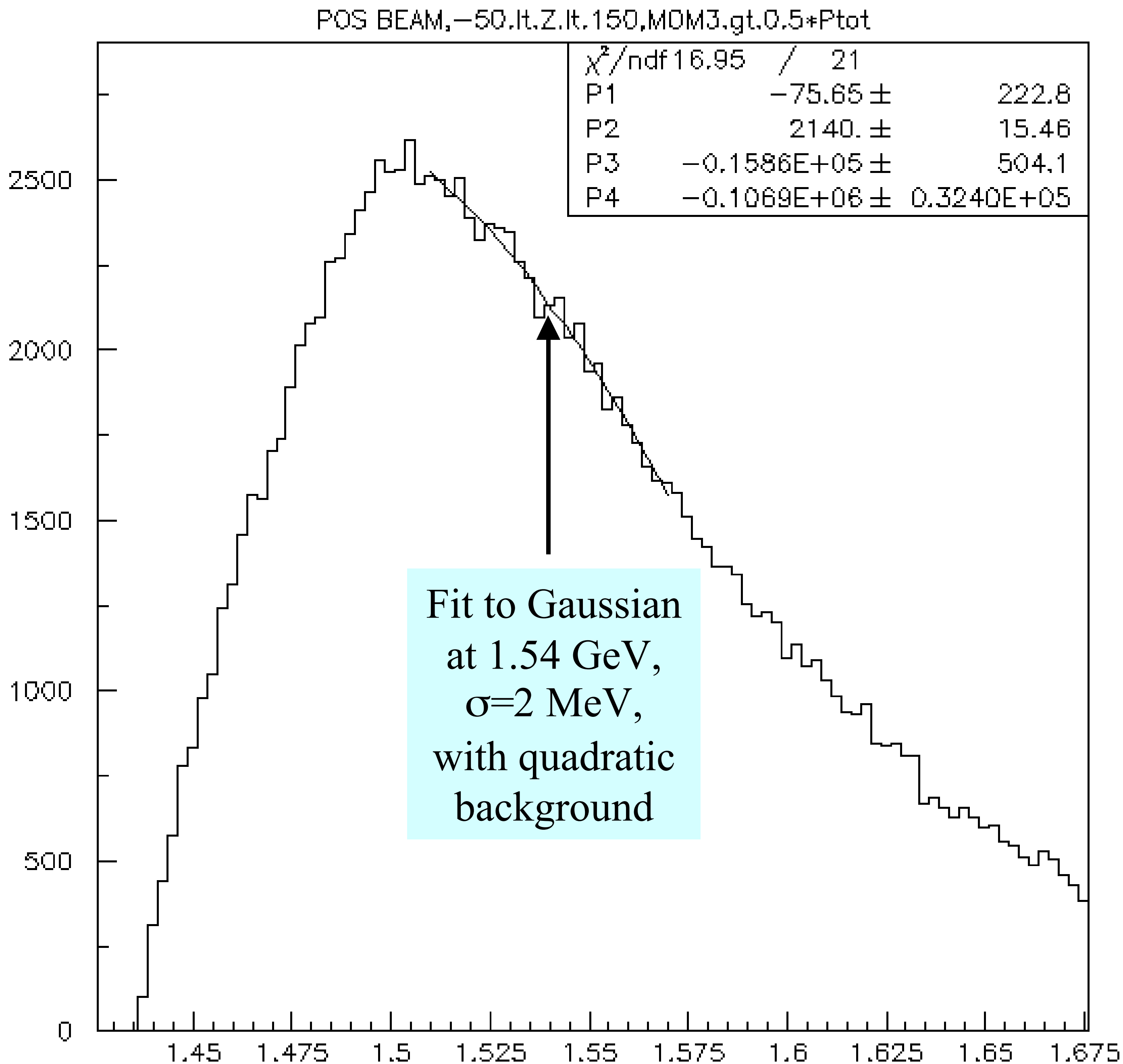

K^0-p mass, either sign

E871/HyperCP, M.Longo @ QNP04

90% CL limit ~370 events out of 150000 K^0-p candidates. P1 is the amplitude of the gaussian. Bins are 2 MeV

HyperCP Preliminary

Pentaquark sightings come from low statistics, low resolution, low-energy experiments with kinematically constrained final states after complicated cuts are imposed.

High resolution, high statisitcs, experiments with both low- and high- particle multiplicity do not report the pentaquarks.

COSY-TOF $pp \to \Sigma^+ K^0_S p$

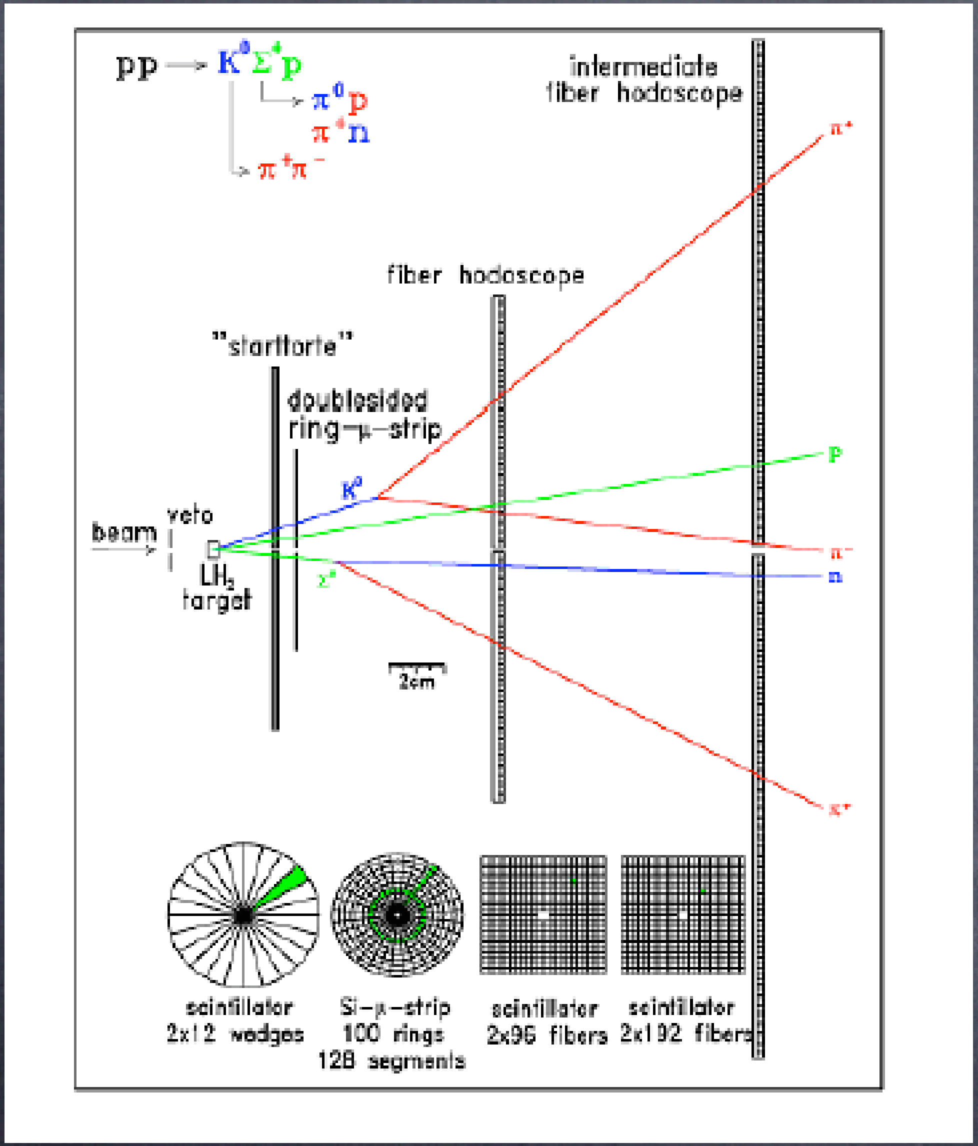

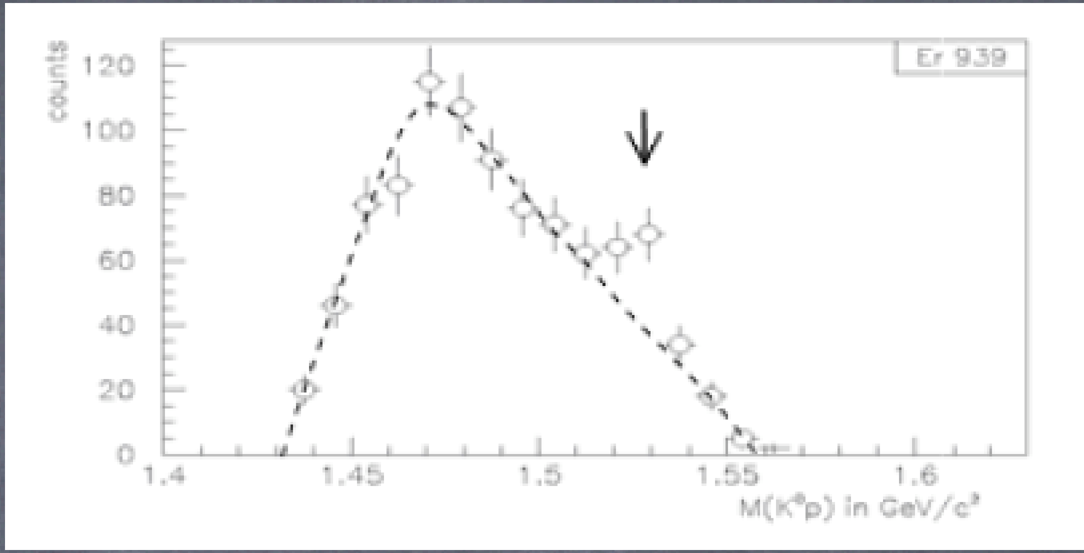

no magnetic filed, PID, pure geometry TOF no used in this analysis !

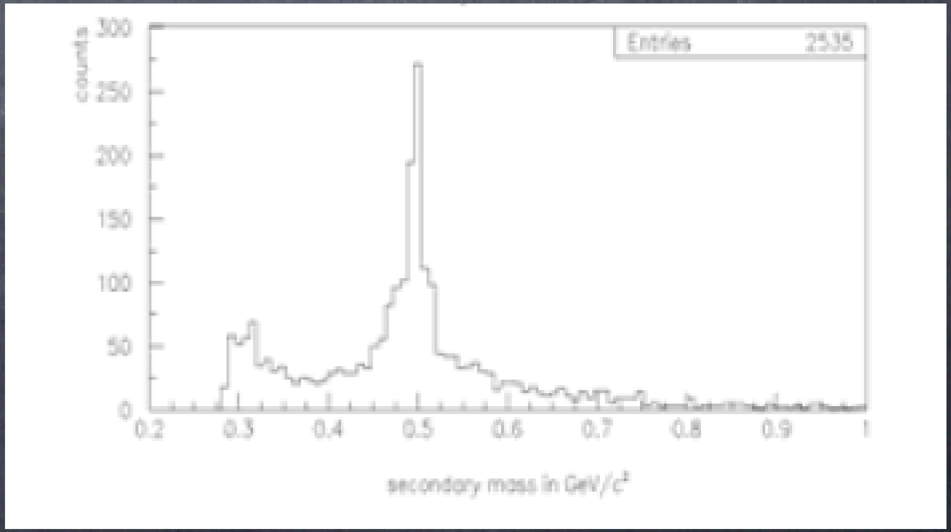

ghost tracks from

$\Xi^- \to \Lambda\pi^- \to p\pi^-\pi^-$ with one π^- reconstructed as 2 tracks

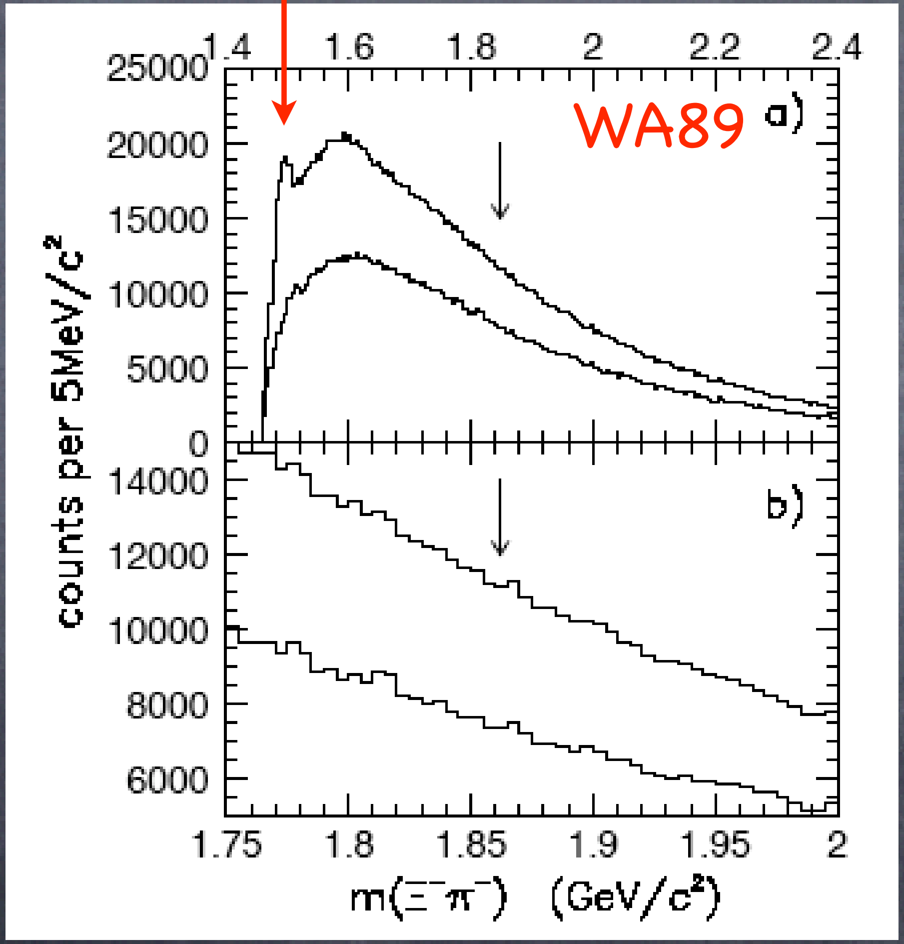

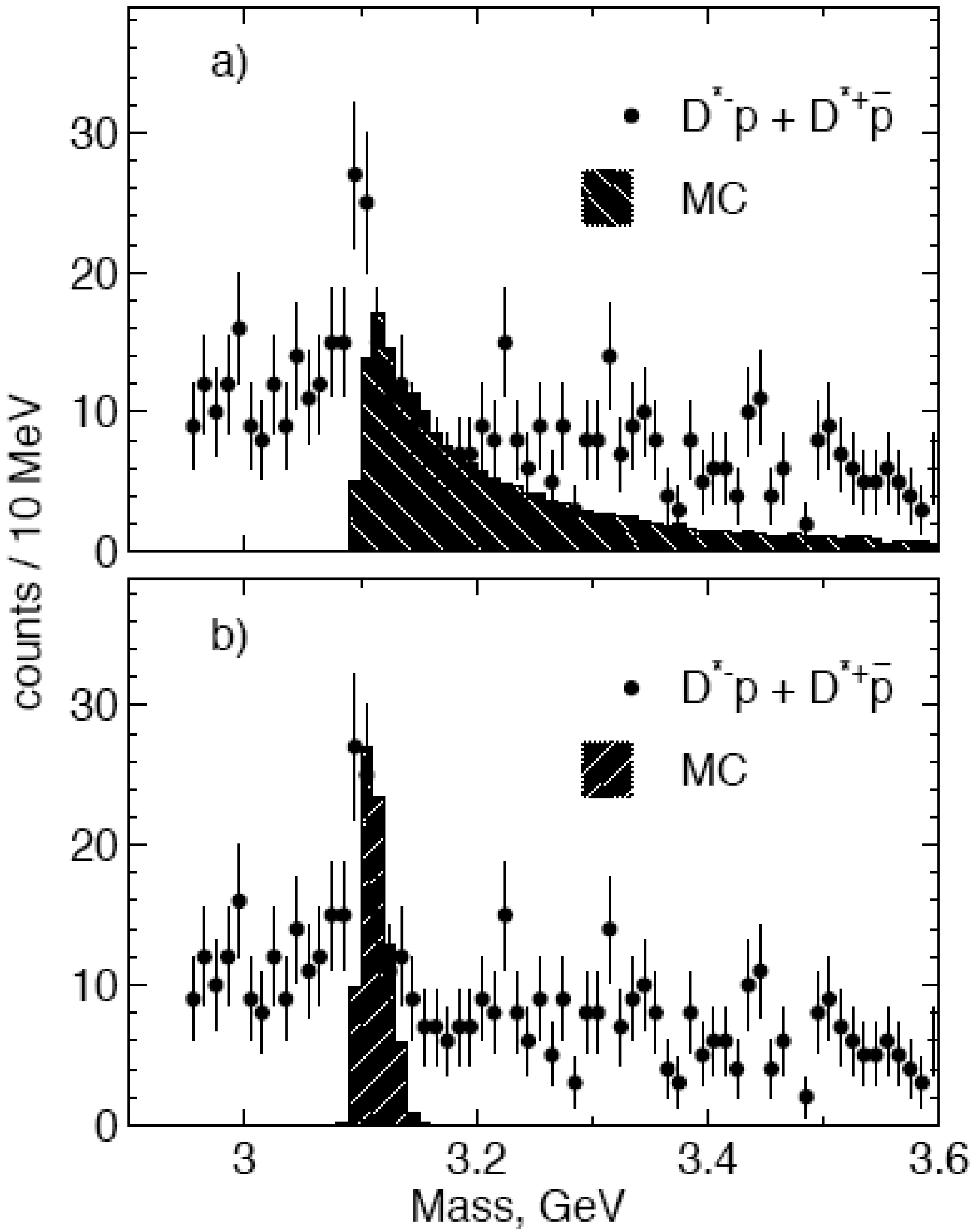

Figure 1: The invariant mass spectra of the $D^{*-}p + D^{*+}\bar{p}$ (taken from [1]) and Monte-Carlo simulation: a) no cut on the "proton" momentum; b) with the cut on the "proton" momentum >20 GeV/c.

The Charm Pentaquark and Kinematic Reflection.

M.Zavertyaev

hep-ex/0501028

$$D^{*+} \rightarrow D^0\pi^+$$

$$\rightarrow K^-\pi^+\pi^+$$

$$K^- \rightarrow K^{-}\text{"}\bar{p}\text{"}$$